nature sustainability

Article

https://doi.org/10.1038/s41893-025-01677-8

Sand-mining-driven reduction in Tonle Sap Lake's critical flood pulse

Received: 2 October 2024

Accepted: 6 October 2025

Published online: 10 November 2025

Check for updates

L. Q. Quan[1,2,3] ✉, C. R. Hackney[4], G. Vasilopoulos[2], T. Coulthard[5], N. N. Hung[3], S. E. Darby[6] & D. R. Parsons[1]

The Tonle Sap Lake (TSL), one of the world's most productive lake–wetland ecosystems is sustained by an annual flood pulse that reverses Lower Mekong River flow into the lake during the monsoon and returns freshwater downstream during the dry season. Recent declines in the reverse flow have previously been attributed to climate change and upstream damming. However, here we show that between 1998 and 2018, riverbed lowering of the Mekong mainstem, driven by sand mining and upstream sediment trapping, has reduced the reverse flow by between 40 and 50% (high- to low-flow year range; 47% for medium flows). Projections to 2038, with additional riverbed lowering driven by ongoing sand mining, predict reverse flow declines of 69% (64–73%) compared with 1998. We show how these changes affect the lake's flow regulation services across the Lower Mekong system. Specifically, the reduced TSL reverse flow increases flows to the Mekong Delta by ~26 km^3 (31–23 km^3) during the monsoon, heightening flood risk, while decreasing dry-season flows by ~59% (50–61%), contributing to intensified saltwater intrusion and diminished agricultural yields across the Mekong's Delta. Our results underscore how excessive sand extraction is an existential threat to the TSL–Mekong system's sustainability.

The Tonle Sap Lake (TSL) is one of the most ecologically diverse lake ecosystems globally and is the fourth most productive in terms of fish productivity[1]. Since 1997, the TSL has been recognized as a UNESCO (United Nations Educational, Scientific and Cultural Organization) World Heritage Biosphere Reserve, serving as a habitat for globally significant populations of endangered amphibians, reptiles, mammals and birds, spanning a diverse array of 885 species[1–4].

The TSL is linked to the Lower Mekong River (LMR) via the Tonle Sap River (TSR), which joins the Mekong at the delta apex in Phnom Penh (Cambodia; Fig. 1a), where the river splits into the LMR and Bassac River, flowing south–southeast to form the Mekong Delta (MD). The Lower Mekong basin (LMB) region's monsoon-driven tropical climate features a wet season (typically mid-May–October), delivering over 90% of annual rainfall[5], and a dry season (November–May). Correspondingly, river discharge and water levels in the LMR generally begin rising in May, peak around September and decline to their annual lows by March[6]. For the majority of the year, fresh water in the TSL drains downstream into the MD via the TSR[6]. However, during the monsoon flood season, water from the Mekong flows back (notionally 'up'stream) into TSL through two main pathways: (1) rising water levels at the delta apex exceed those in the lake, creating a hydraulic gradient that causes the flow of the TSR to reverse, driving water from the LMR into the TSL[7]; (2) the Mekong floods onto the Tonle Sap floodplain (TSF; right bank of the LMR from Kompong Cham to Chaktomuk; Fig. 1a), with about half the overland flow entering the lake directly and the rest via the TSR[8]. This seasonal flow reversal typically raises the lake's water level (measured at Kompong Luong during 1997–2005) from a dry-season average minimum of 1.32 m (standard deviation

[1]Geography and Environment, Loughborough University, Loughborough, UK. [2]Energy and Environment Institute, University of Hull, Hull, UK. [3]Southern Institute of Water Resources Research, Ho Chi Minh City, Vietnam. [4]School of Geography, Politics and Sociology, Newcastle University, Newcastle-upon-Tyne, UK. [5]Department of Natural Sciences, Manchester Metropolitan University, Manchester, UK. [6]School of Geography and Environmental Science, University of Southampton, Southampton, UK. ✉e-mail: q.le@lboro.ac.uk

https://doi.org/10.1038/s41893-025-01677-8

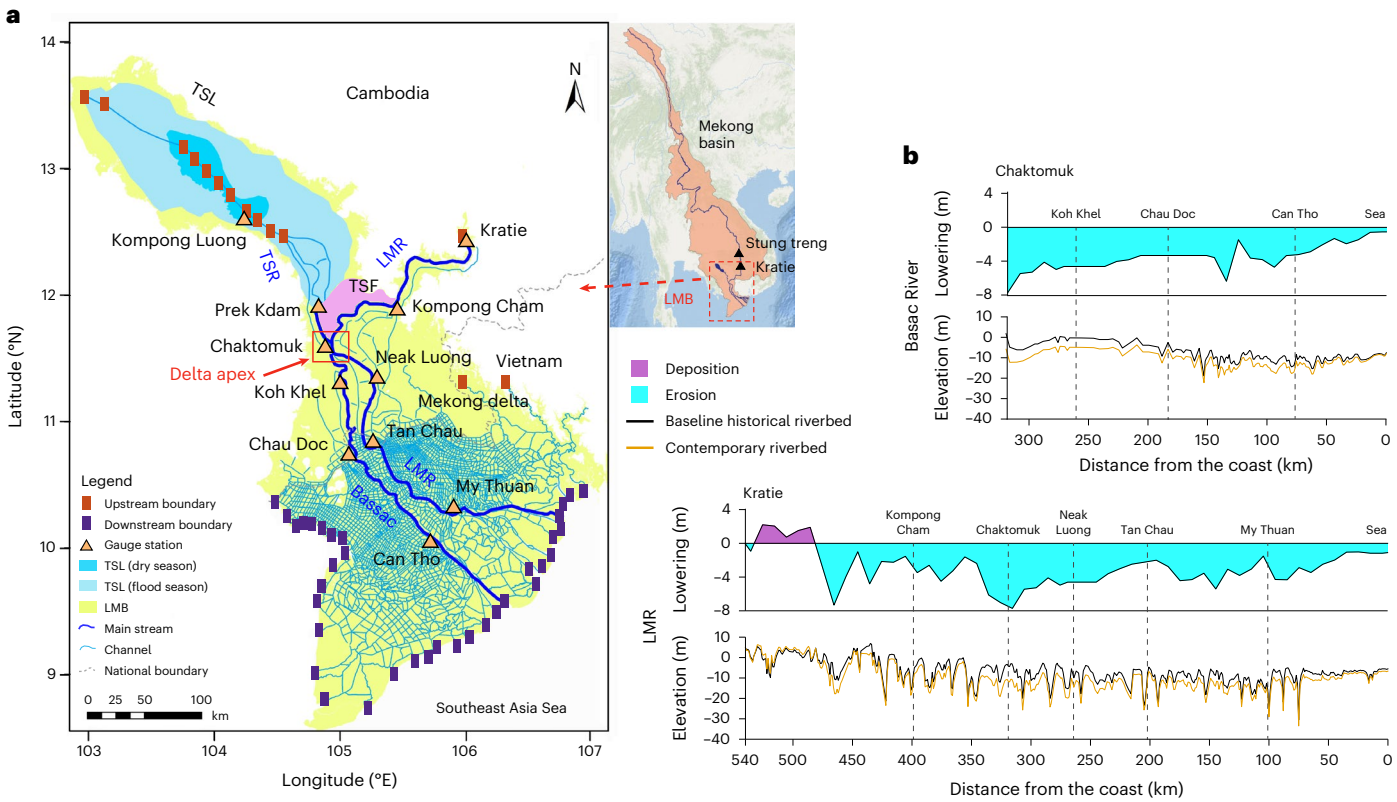

Fig. 1 | 1D model domain and observed riverbed lowering in the LMB. a, 1D model domain of the LMB, including the LMR, the TSF (highlighted in light purple; situated in the southwestern area of the LMR, adjacent to TSL), TSL, TSR and MD and identifying key gauge locations in the LMB. **b**, Observed laterally averaged riverbed elevations and the averaged changes in depth along the Bassac River (top) and the LMR (bottom) for the baseline historical and contemporary bathymetries (from refs. 28,30; Methods). Credit: basemaps in **a**, Esri, USGS | Esri, TomTom, FAO, NOAA, USGS.

(σ) = 0.10 m) to a flood-season peak of 9.14 m (σ = 1.00 m) above Ha Tien mean sea level (m.s.l.)[7,9]. Consequently, the lake's surface area expands by an order of magnitude, from 2,210 km^2 (σ = 118 km^2) to approximately 13,260 km^2 (σ = 1,714 km^2), with the volume of the lake experiencing an even greater increase from around 1.6 km^3 (σ = 0.2 km^3) up to 59.7 km^3 (σ = 13.0 km^3) (refs. 7,9). Overall, approximately 57% of the lake's water originates from the LMR, with around 52% entering through the TSR and ~5% entering directly through the TSF, with Tonle Sap basin tributaries contributing an additional 30% and direct precipitation accounting for the remaining 13% (all data are for the 1997–2003 period)[7].

The flow reversal and TSL function as a vast water capacitor for the MD, storing sufficiently large volumes of the Mekong's seasonal floodwater to modulate down flood-season water levels across the MD, and then releasing the stored water during the dry season to augment base flows in the delta[8,10]. As such, the lake's flood-pulse functioning is not just critical in terms of sustaining the lake's biological productivity and biodiversity but is also integral to regulating water systems and water levels across the entire lower Mekong system.

However, recent observations have highlighted changes in the timing and (reduced) duration of the reverse flow into the TSL, reducing the lake's seasonal inundation and raising concerns that the normal functioning of the annual reverse flow is becoming compromised[11–16]. Specifically, the average annual reverse flow volume from the LMR into TSL (measured at Prek Kdam on the TSR) decreased from 41.5 km^3 during 1996–2009 (midpoint 2003) to 29.3 km^3 during 2010–2024 (midpoint 2017), representing a 29.4% decline over 14 years[17]. Consequently, maximum water levels in the lake (measured at Kompong Luong) dropped by 1.05 m on average between 2010 and 2019 compared with 1996–2009[14], while the average maximum annual inundated area decreased by 16.4%, from 11,917 km^2 (2001–2009) to 9,967 km^2 (2010–2020)[16].

Although inter-annual changes in the timing and duration of the reverse flow into the TSL may be driven by natural hydro-climatic variability, the causes behind the declining trend in reverse flow and the associated shrinking of the TSL remain unclear. Previous studies have suggested that these declines may variously be attributed to (1) reductions in flood magnitudes on the LMR due to climate change[16,18,19] and (2) reductions in flood season water levels on the LMR due to flow regulation by upstream dams[15,20] and urban development (projects for irrigation, flood control, domestic water supply) in the Mekong basin[11,16]. However, rainfall and flow measurements do not support these explanations. Recorded rainfall in the Cambodian floodplains has remained relatively stable between 1960 and 2019[14,21]. The influence of dam operations in both the upper Mekong and the LMB on flows within the LMR, and especially at the delta apex, is also considered limited[13,19,22]. For example, upstream run-off changes have had minimal effects on flows at Stung Treng (~120 km upstream of Kratie; Fig. 1a), with only slight seasonal variations between 2000 and 2014[23], and long-term water-level data at Stung Treng show no significant trends in flood peaks or duration from 1960 to 2019[14] (Supplementary Table 7). Likewise, discharge records from the TSR at Prek Kdam and the LMR at Chaktomuk (Fig. 1a) indicate that only ~8% of the decline in reverse flow can be attributed to upstream hydrograph changes on the Mekong[14]. This means that the observed decline in the reverse flow into the TSL cannot be explained by hydrological factors alone and instead must be driven by other factors too.

One such alternative factor may be the role of changes in the morphology of the Mekong riverbeds around and beyond the delta apex (Fig. 1b). Specifically, if systematic riverbed lowering is occurring, this

could lower flood-season water levels in the LMR[24], thereby reducing the hydraulic gradient between the delta apex and TSL, and potentially also decrease the floodwater flow from the LMR into the lake. In fact, recent studies show substantial sediment loss in the Mekong River due to dam-induced trapping, with 283 large hydropower projects either operational or under construction[25]. Sediment deficits are being further exacerbated by intense rates of sand mining in the LMR and its delta[26–30]. In 2020, Cambodia extracted 59 Mt of sand[30], nearly double the 32 Mt in 2011[26] and far exceeding the estimated natural sand influx of 6.18 ± 2.01 Mt yr^{-1}(ref. 31). In the Vietnamese part of the MD (VMD), sand mining averaged 42 Mm^3 yr^{-1} (around 67.2 Mt yr^{-1}) between 2015 and 2020[29]. These combined impacts have led to substantial riverbed lowering, with rates of 0.26 m yr^{-1} observed during 2013–2019 in Cambodia[30] and a lowering rate of 0.16 m yr^{-1} observed across the VMD during 2008–2018[28].

We therefore propose here that the observed reductions in the intensity of the TSR's reverse flow are being driven predominantly by substantial recent lowering of the LMR's bed elevation in the vicinity of, and beyond, the delta apex. We argue that the consequent impacts on water levels on the LMR are sufficiently large to affect the water surface gradients between the delta apex and the lake that drive the TSR reverse flow. We test this hypothesis by employing a numerical model to quantify changes of the TSR flow reversal in response to varying levels of riverbed lowering of the mainstem LMR and assess the significance of these diminished flow reversals in terms of region-wide provisioning and regulating ecosystem services.

Results

A one-dimensional (1D) hydrodynamic model, MIKE 11, is employed to simulate the flow dynamics throughout the entire river network of the LMB between Kratie, the TSL and the MD, using mainstream bathymetric data from 1998 (Fig. 1a). The model's upstream boundary is controlled by daily water discharge data at Kratie in the LMR along with 11 boundary inputs from the Tonle Sap Basin within the TSL (Fig. 1a; see Extended Data Fig. 4 for names and exact locations), while downstream boundary conditions along the coastal Mekong area utilize tidal elevations with an hourly resolution (Fig. 1a and Methods). The model, calibrated for high water-flux conditions for the year 2000 (in which the water volume passing through Kratie was 523 km^3) and validated with low water-flux data from 2003 (328 km^3), shows strong agreement with observed water levels across the main river gauging stations (Methods). In addition, further validation confirms the model's capability to capture the effects of historical riverbed lowering on observed system-wide water-level reductions, particularly at the delta apex (Methods).

A total of nine scenarios were simulated with the calibrated model, representing a range of riverbed lowering magnitudes and imposed flows (Extended Data Fig. 7a–c and Methods). Specifically, we simulated three magnitudes of riverbed lowering: (1) a baseline historical scenario where zero riverbed lowering was assumed on the basis of bathymetric data measured in 1998; (2) a contemporary scenario where riverbed levels were reduced by an average of 3.06 m (σ = 2.03 m), based on observed bed lowering between 1998 and 2018; and (3) a potential future scenario projection of river bathymetry based on ongoing bed lowering at current rates for 20 more years (to 2038), resulting in an average reduction of 5.92 m (σ = 2.84 m) compared with 1998 (Methods). These three bed-level scenarios were combined with three forcing hydrograph scenarios at the model's upstream boundary that represent (1) low (total water volume of 301 km^3), (2) medium (415 km^3) and (3) high (500 km^3) water-flux conditions. Although these three flow scenarios were developed using observed water discharge conditions for the years 2010, 2009 and 2011, respectively (Methods), we emphasize that the selected flows are intended to encompass a wide, but realistic, range of imposed flow variabilities rather than replicating specific historical conditions. Importantly, this range of imposed flows not only represents past hydro-climatic variability, but encompasses the range of flows projected under future climate change and basin development (Methods). All simulated water discharge and water levels are extracted as daily values, with water levels referenced to the Hon Dau m.s.l. (Methods).

Changes in the TSR flow reversal

Our results show that Mekong River bed lowering reduces the total volume of water flowing from the LMR to the TSL, as estimated at Prek Kdam, through both the TSR and the TSF (red bars, Fig. 2a–c). Specifically, for the medium water-flux year, the total simulated reverse flow from the LMR into the TSL in the baseline historical scenario is 45.1 km^3. Of this total volume, about 36.0 km^3 is contributed by the TSR, while 9.1 km^3 comes from the TSF via overland flow. Under the contemporary (average riverbed lowering of −3.06 m) scenario, this total flow decreases to 24.0 km^3 (21.3 km^3 from the TSR and 2.7 km^3 from the TSF), a 46.8% reduction compared with the baseline historical scenario (Fig. 2b). Finally, for the future (average riverbed lowering of −5.92 m) scenario, the projected simulated inflow further declines to 13.9 km^3 (13.2 km^3 from the TSR and 0.7 km^3 from the TSF), representing a 69.3% decrease in total inflow volume to the TSL compared with the baseline historical scenario (Fig. 2b). Similar decreases are observed in our simulations for the low and high water-flux years (Fig. 2a–c and Extended Data Table 1).

The reduction in total reverse water fluxes is mirrored in a reduction in the maximum flow discharges (estimated at Prek Kdam) flowing into the TSL. Specifically, for the medium water-flux year, the simulated peak discharge to the TSL in the baseline historical scenario is 9,084 m^3 s^{-1}, a value that decreases to 5,390 m^3 s^{-1} in the contemporary scenario (40.7% reduction) and to 3,675 m^3 s^{-1} (59.5% reduction) in the future scenario (Fig. 2e). In addition to reduced peak discharges, the simulated duration of the reverse flow is also shortened. For the medium water-flux year, the reverse flow lasts 136 days in the baseline historical scenario but only 121 days (11% decrease) and 91 days (33.1% decrease) in the contemporary and future scenarios, respectively (green bars; Fig. 2b). These trends are broadly similar for the low and high water-flux years (Fig. 2a–f and Extended Data Table 1).

Changes in TSL water level and inundation area

As the simulated inflow of water from the LMR into the TSL declines with the progressive riverbed level lowering in the main rivers of the LMB, there is a reduction in both the flood-season water level simulated in the TSL and the extent and duration of inundation (Fig. 3a–i and Extended Data Table 2). For the medium water-flux year, the maximum simulated water level in the TSL (at Kompong Luong) is 8.63 m under the baseline historical scenario. This water level declines to 6.66 m under the contemporary scenario, marking a sharp decline of 1.97 m, and further to 5.42 m in the future scenario, representing a decrease of 3.21 m compared with the baseline historical condition (Fig. 3b).

The reduction in peak lake water levels leads to a corresponding decline in the estimated maximum spatial extent of TSL inundation (Methods, Fig. 3b and Extended Data Table 2). For the medium water-flux year, the maximum flooded area of the TSL is estimated to be 12,653 km^2 for the baseline historical scenario but decreases to 9,525 km^2 in the contemporary scenario (a reduction of 3,128 km^2 or 24.7% compared with the baseline historical scenario) and just 7,624 km^2 in the future scenario (a reduction of 5,029 km^2 or 39.7%).

The simulated declining trends in flood-season water level and inundation extents are reflected also in the simulated duration of specified inundation extents (Fig. 3g–i). The impacts on the TSL flood extent can be quantified by comparing the amount of time the TSL is inundated beyond the long-term average flooded area value (A_f; 6,153 km^2 as calculated for the period 1998 to 2021; Methods). For the medium water-flux year, A_f is predicted to be exceeded for 213 days under the baseline historical condition, but this duration decreases

https://doi.org/10.1038/s41893-025-01677-8

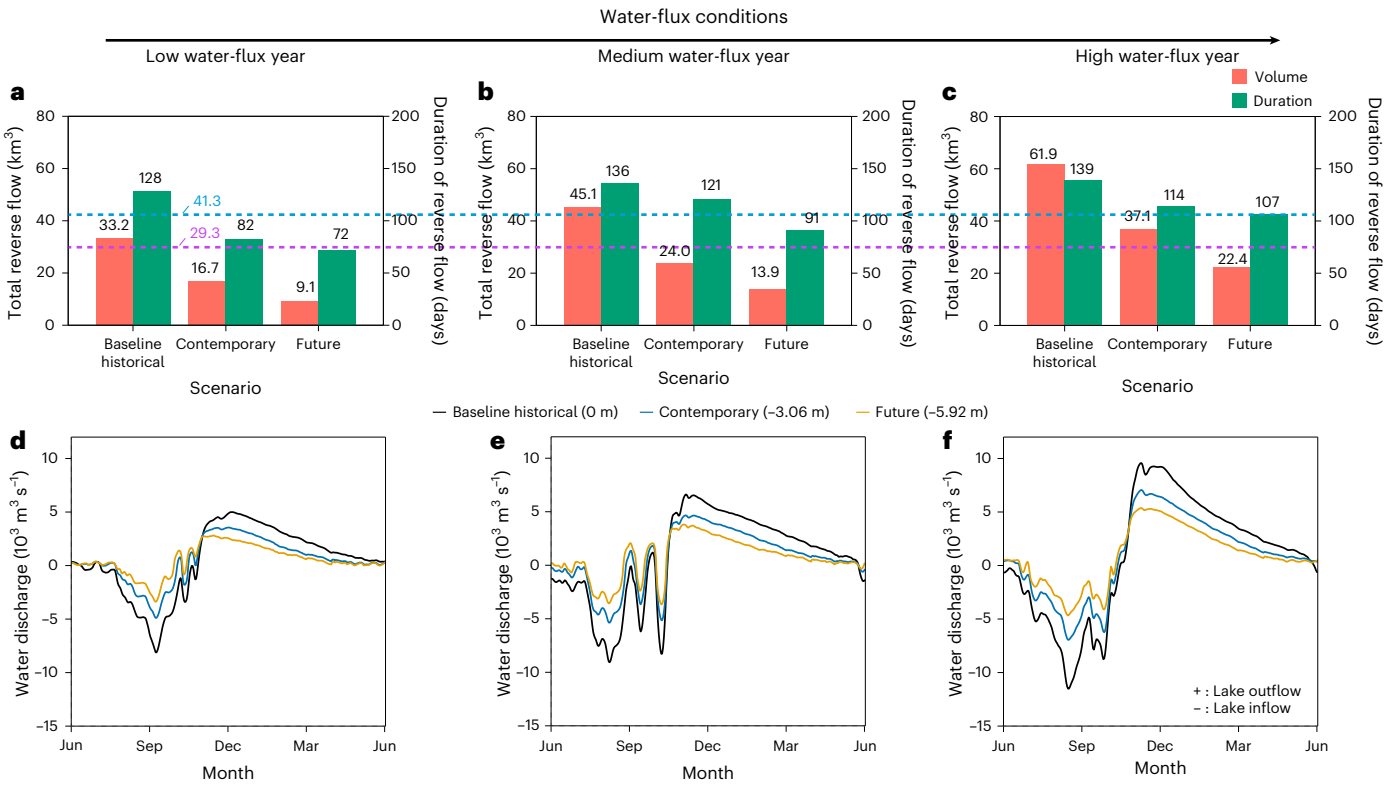

Fig. 2 | Hydrological impacts of riverbed lowering on Tonle Sap reverse flow. **a**–**c**, Simulated total volume of reverse water flowing from the LMR to the TSL and the cumulative duration of reverse flow into the TSL for the baseline historical (0 m), contemporary (−3.06 m) and projected future (−5.92 m) riverbed level bathymetries under low (**a**), medium (**b**) and high (**c**) water-flux years, with all data estimated at Prek Kdam. The blue and the purple dashed lines depict the average annual reverse flow volume from the LMR to the TSL (as calculated at Prek Kdam) calculated by the MRC[17] during the periods 1996–2009 and 2010–2024, respectively. **d**–**f**, Simulated daily water discharge (at Prek Kdam) under the different scenarios of riverbed lowering and various hydrograph conditions: low water flux (**d**), medium water flux (**e**) and high water flux (**f**). Negative values indicate a reverse flow of the TSR (that is, from the LMR into the TSL).

to 148 days and 99 days for the contemporary and future scenarios, respectively. These are large reductions of 65 days and 114 days, respectively (Fig. 3h). These simulated declines are so pronounced that our predictions indicate that maximum inundation area of the lake will, in low water-flux years, no longer attain the mean flooded area value A_f in the future scenario (Fig. 3g). Full results for the other upstream forcing hydrographs are shown in Fig. 3a–f and Extended Data Table 2.

Changes in water fluxes into the Mekong Delta

Our model projections show that there are increased water flows into the MD (that is, the sum of the water fluxes directed into the Mekong and Bassac rivers downstream of the delta apex; Fig. 1a) during the flood season (June to November, as per the definition of the Mekong River Commission (MRC)[32]). Focusing on the medium water-flux year (with data for the low and high water-flux years shown in Fig. 4a–i and Table 1), the total simulated water volume flowing from the delta apex into the MD is 289.8 km^3 in the baseline historical scenario, increasing to 328.8 km^3 (a 13.5% increase relative to the baseline historical bathymetry scenario) and 346.7 km^3 (a 19.6% increase) in the contemporary and future scenarios, respectively (Fig. 4b and Table 1).

These model-simulated increases in flood-season flows into the MD are attributed to two factors: (1) increased flow within the LMR upstream of the delta apex, as riverbed lowering enhances channel conveyance and lowers water levels (Extended Data Fig. 1a–c and Supplementary Tables 5 and 6), thereby reducing floodwater storage on the adjacent floodplains (between Kratie and the delta apex; Fig. 1a) and (2) a loss of (Mekong-sourced) floodwater storage in the TSL due to the weakened seasonal reversal of the TSR, also driven by riverbed lowering. Specifically, the total simulated water volume flowing from the LMR to the delta apex (for a reference location directly upstream of the apex, Fig. 1a) is 281.9 km^3 in the baseline historical scenario, a value that increases to 332.2 km^3 (14.7% increase) and 340.1 km^3 (20.7% increase) in the contemporary and future bathymetry scenarios, respectively (Fig. 4e and Table 1). Meanwhile, the total flood-season water volume simulated flowing from the LMR to the TSL (at Prek Kdam) is 21.4 km^3 in the baseline historical scenario. However, this volume decreases to 4.8 km^3 (a decrease of 77.5%) and −4.4 km^3 (a 120% decrease or an additional flood-season flow from TSL to the delta apex of 25.8 km^3 relative to the baseline historical scenario) in the contemporary and future bathymetry scenarios, respectively (Fig. 4h and Table 1). The negative value for the future scenario indicates that there is a net outflow from the TSL to the LMR during the flood season (June to November) as the TSR continues to reverse for a brief period in this scenario, but the duration and magnitude of the flow is substantially reduced.

Our model projections also show that there are decreased water flows into the MD during the dry season (December to May). Focusing on the medium water-flux year (with corresponding data for the low and high water-flux years presented in Fig. 4a–i and Table 2), the total water volume flowing from the delta apex into the MD is simulated at 107.8 km^3 for the baseline historical scenario, reducing to 92.4 km^3 (a decline of 12.6% relative to the baseline historical bathymetry scenario) and 85.6 km^3 (a 20.6% decrease) in the contemporary and future scenarios, respectively (Fig. 4b and Table 2).

As with the flood-season flows, these decreased water flows into the Mekong Delta are driven by the sum of the changes in water fluxes flowing (1) from the LMR (upstream of the apex) to the delta apex (Fig. 4b and Table 2), but in the dry season, and (2) from the TSL towards the delta apex (Fig. 4b and Table 2). Of these two effects, our model results

https://doi.org/10.1038/s41893-025-01677-8

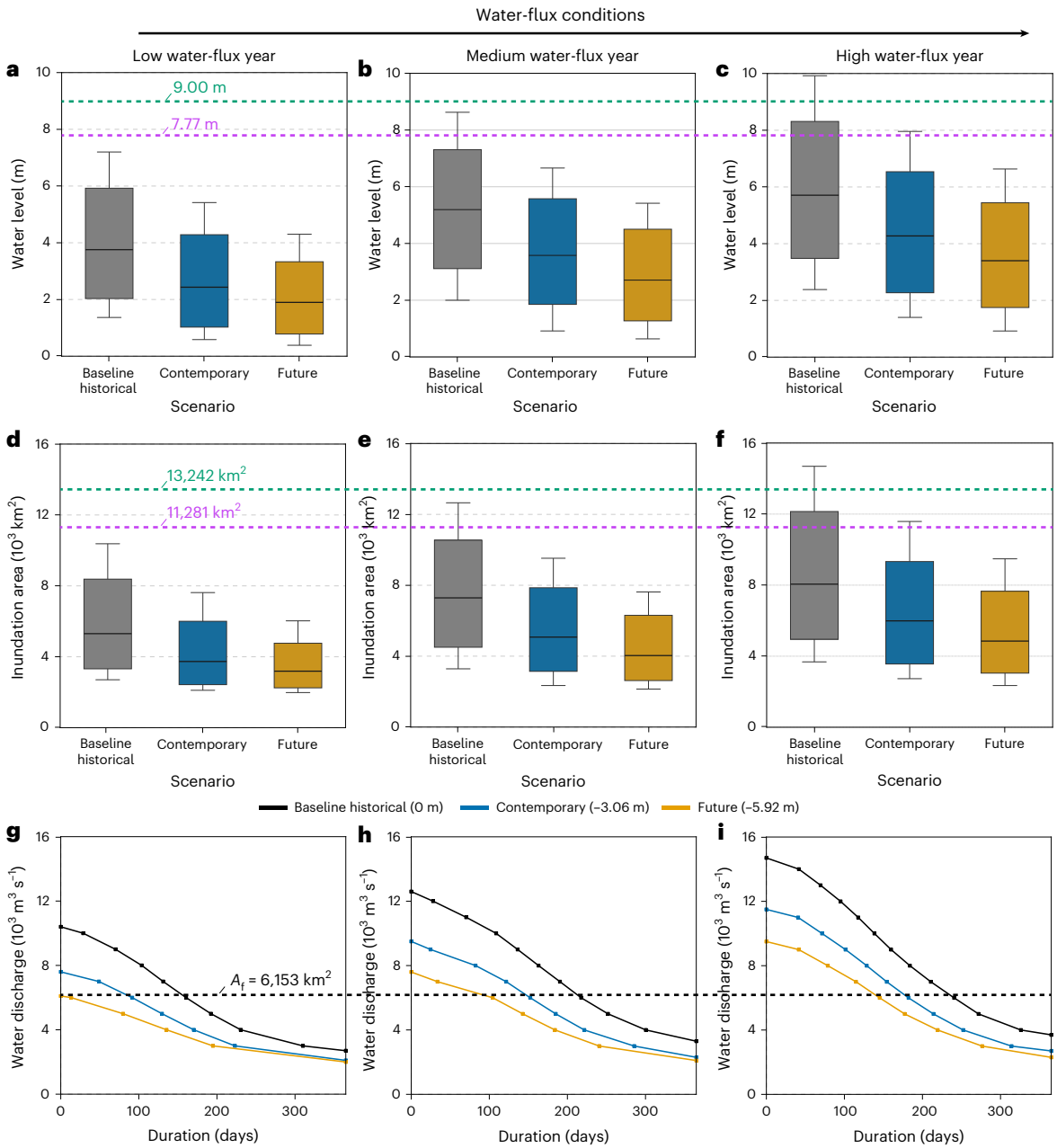

Fig. 3 | Hydrological impacts of riverbed lowering on TSL water level and inundation. a–**c**, The daily simulated water levels within TSL (at Kompong Luong gauge, referenced to Hon Dau m.s.l.; $n = 365$ daily simulated water levels) over a 1-year simulation period for the baseline historical, contemporary and projected future bathymetries under low (**a**), medium (**b**) and high (**c**) water-flux years. In each box plot, the central line represents the median daily water level, the box bounds indicate the 25th–75th percentiles (with 25% and 75% of daily water levels falling below these values, respectively), and the whiskers show the full range of simulated daily water levels (minimum to maximum). **d**–**f**, Simulated inundation areas within TSL (calculated from daily simulated water level at Kompong Luong gauge; Methods; $n = 365$ daily calculated inundation area values) over a 1-year simulation period for the baseline historical, contemporary and projected future bathymetries under low (**d**), medium (**e**) and high (**f**) water-flux years. In each box plot, the central line represents the median daily inundation area, the box bounds indicate the 25th–75th percentiles (with 25% and 75% of daily inundation areas fall below these values, respectively), and the whiskers show the full range of simulated daily inundation areas (minimum to maximum). **g**–**i**, The relationship between the magnitudes and durations of inundation areas within the TSL under the three bathymetry conditions and hydrograph scenarios: low water flux (**g**), medium water flux (**h**) and high water flux (**i**). The black dashed line represents the long-term average flooded area (A_f) as calculated for the period 1998–2021 (Methods).

indicate that the second dominates over the first. Specifically, for the medium water-flux year, the total water volume flowing from the LMR to the delta apex is 64.6 km^3 in the baseline historical scenario, increasing slightly to 67.1 km^3 (a 3.8% increase) and 67.5 km^3 (a 4.4% increase) in the contemporary and future bathymetry scenarios, respectively. However, the simulated total volume of water flowing from the TSL to the delta apex during the dry season decreases substantially from 43.9 km^3 in the baseline historical scenario to 27.3 km^3 (a 37.8% decrease) and 18.2 km^3 (a 58.7% decrease) in the contemporary and future bathymetry scenarios, respectively. These reductions in dry-season lake outflows are driven by there simply being less water to drain from the lake in the dry season following the reduced flood-season infilling.

Discussion

Our results indicate that anthropogenically induced riverbed lowering in the LMR increases channel conveyance, reducing flow to the TSF and

https://doi.org/10.1038/s41893-025-01677-8

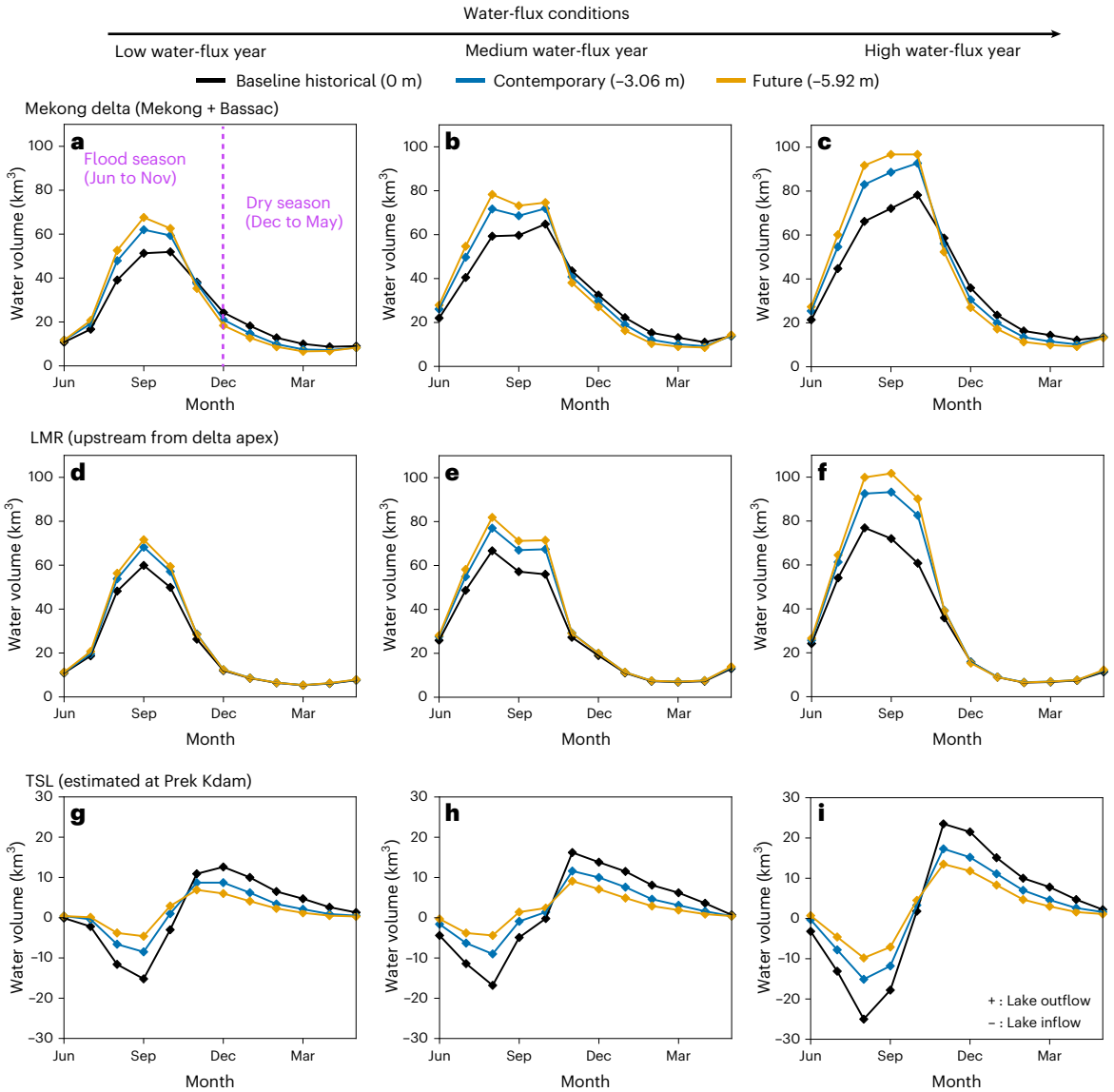

Fig. 4 | Hydrological impacts of riverbed lowering on water fluxes into the Mekong Delta. a–i, The simulated monthly water volumes flowing from the delta apex to the MD (via the LMR and Bassac River) (**a**–**c**), from the LMR to the delta apex (with discharge extracted immediately upstream of the delta apex) (**d**–**f**) and from the LMR into the TSL (estimated at Prek Kdam) (**g**–**i**) under different riverbed lowering scenarios and for low (**a**,**d**,**g**), medium (**b**,**e**,**h**) and high (**c**,**f**,**i**) water-flux years, respectively.

Table 1 | The total water volume from the delta apex to the MD (via the LMR and Bassac River), from the LMR to the delta apex and from the LMR to the TSL (estimated at Prek Kdam) under different freshwater flux conditions and riverbed lowering scenarios during the flood season from June to November

	Delta apex to MD (km^3)			LMR to delta apex (km^3)			LMR to TSL (km^3)		
	Baseline	Contemporary	Future	Baseline	Contemporary	Future	Baseline	Contemporary	Future
Low flux	208.0	237.7 (14.3%)	250.5 (20.5%)	213.8	238.7 (11.6%)	247.1 (15.8%)	21.2	5.4 (–74.8%)	–1.9 (–109.0%)
Medium flux	289.8	328.8 (13.5%)	346.7 (19.6%)	281.9	332.2 (14.7%)	340.1 (20.7%)	21.4	4.8 (–77.5%)	–4.4 (–120.4%)
High flux	341.2	400.4 (17.4%)	424.8 (24.5%)	324	394.5 (21.8%)	421.9 (30.2%)	33.8	14.4 (–57.2%)	2.9 (–91.4%)

Percentages in parentheses indicate changes relative to the baseline historical scenario, with negative values representing reductions.

lowering water levels at the critical delta apex (Extended Data Fig. 1a–c). In turn, this weakens the hydraulic gradient that drives the flood-season flow reversal into the TSL.

Our simulations show that, in a medium water-flux year and compared with the 1998 bathymetry conditions, ongoing riverbed lowering by 2038 could reduce the total Mekong water flow to the TSL by about 69% (64–73%), with the values in parentheses referring to high and low water-flux years, respectively. These hydrological changes would also reduce the lake's maximum inundation area by ~40% (35–42%) and decrease the vital return flows to the MD in the dry season (December to May) by close to 59% (50–61%), with a consequent reduction of around 21% (24–26%) in the dry-season water flux from the delta apex to the

https://doi.org/10.1038/s41893-025-01677-8

Table 2 | The total water volume from the delta apex to the MD (via the LMR and Bassac River), from the LMR to the delta apex and from the TSL to the delta apex (estimated at Prek Kdam) under different freshwater flux conditions and riverbed lowering scenarios during the dry season from December to May

	Delta apex to MD (km^3)			LMR to delta apex (km^3)			TSL to delta apex (km^3)		
	Baseline	Contemporary	Future	Baseline	Contemporary	Future	Baseline	Contemporary	Future
Low flux	82.9	68.7 (–17.1%)	61.6 (–25.6%)	45.8	47 (2.7%)	47.1 (2.8%)	37.7	21.8 (–42.1%)	14.5 (–61.4%)
Medium flux	107.8	92.4 (–12.6%)	85.6 (–20.6%)	64.6	67.1 (3.8%)	67.5 (4.4%)	43.9	27.3 (–37.8%)	18.2 (–58.7%)
High flux	115.8	99.2 (–14.4%)	87.8 (–24.2%)	56.6	57.6 (1.8%)	57.6 (1.8%)	61.3	42.1 (–31.4%)	30.5 (–50.3%)

Percentages in parentheses indicate changes relative to the baseline historical scenario, with negative values representing reductions.

MD (Tables 1 and 2). The percentage reduction of dry-season water flux to the MD under medium water-flux conditions is smaller than that for the high water-flux year because, in the dry season, the total water volume from the delta apex to the MD is greater, resulting in a smaller proportional decrease (Table 2). Importantly, the simulated reductions in reverse flow to the TSL during the flood season (June to November) also mean that, independent of any change in discharge in the LMR upstream of the delta apex, an additional ~26 km^3 (31–23 km^3), of water would be transmitted into the delta at a time of already high water levels. Taken together, these changes in the dynamics of the TSR flow reversal potentially have profound consequences, not only for the biological productivity of the TSL but for flow regulation services across the entire LMR and delta system, as considered further in the following.

Given the well-established links between hydraulic regime, ecosystem services and fish production in the TSL[3,20], a decrease in the reverse flow from the LMR to the TSL has the potential to trigger a variety of damaging socioecological impacts, affecting the nearly two million people in Cambodia who depend on the TSL for their livelihoods[4,20]. In particular, the reduced water volumes entering the TSL would probably lead to a decline in migratory fish populations[33,34], which account for 63% of the overall fisheries catch in the TSL[35]. Indeed, recent trends in the total fish catch across 110 species suggest there has already been an 88% decline during the period from 2003 to 2019[34].

In addition, since the LMR is a key nutrient source for the TSL[36], a substantially reduced reverse flow could limit the supply of sediment-bound nutrients, which are increasingly valuable due to upstream dam-related declines in sediment flux. This sediment-bound nutrient reduction could harm spawning site productivity, negatively affecting agriculture and fish production[20,33]. Moreover, the decrease in the lake's inundated areas (Fig. 3d–f) could impact protected flooded forest ecosystems, disrupting plant communities and biodiversity, affecting the habitats of amphibians, reptiles and birds in these flooded areas[3,37]. However, the sediments and nutrients that do not reach the TSL will benefit downstream ecosystems and communities in the MD. This trade-off reflects the interconnectedness of sediment dynamics across the LMB and the mutual dependencies between Cambodia and Vietnam.

The decrease in the volume of water supplied by the TSL to the delta during the dry season (Fig. 4g–i) may also give rise to new water-related challenges in the MD, in particular by limiting freshwater availability for rice cultivation and by threatening aquaculture viability, notably through a very substantial increase in tidal ingress and saline intrusion[28,38]. In addition, the increased flood-season flow from the TSL into the MD during a time of already elevated flood levels would exacerbate flood hazards in the MD.

The only effective mitigation for these problems is to halt and reverse the riverbed lowering that we show is the primary cause of disruption to the TSR reverse flow. This could be achievable by creating positive sediment budgets for the LMR through actions such as restricting or ceasing riverine sand mining[31] and by facilitating the release of sediment that is currently trapped behind dams, through flushing[39,40]. One possible approach is the 'turbidity current venting' method[39], successfully implemented in the Yellow River[39,41], which flushes sediments during floods by directing dense, sediment-laden currents along the reservoir bottom towards the dam. Applying this technique for existing or projected future dams on the Mekong could help mitigate the impacts of riverbed lowering. However, sediment flushing faces technological, socioecological and financial constraints, and releases primarily fine sediments, which are likely insufficient to restore the coarse sands needed to limit riverbed lowering, highlighting the need for basin-wide, coordinated sediment management.

Our findings underscore the persistent environmental consequences resulting from riverbed lowering induced by upstream dams and intensive sand mining in the LMB, an issue shared by numerous river deltas globally that are undergoing rapid economic development[42,43]. As pressures for sand, hydropower and fresh water intensify, it is crucial that sustainable policies prioritize sediment management and foster collaborative governance of transboundary river systems[44].

Methods

Hydrodynamic numerical models are essential tools for analysing flow dynamics and water movement in river deltas and coastal regions, offering a robust framework to simulate natural and human impacts on deltaic hydraulic regimes across scales[45,46]. In particular, hydrodynamic models are effective for assessing how riverbed lowering, caused by activities such as sand mining, dam-induced sediment trapping and dredging, can lead to reduced water levels in rivers and their deltas[47–50]. In this study, a 1D hydrodynamic model covering the entire LMB was used to simulate water-level changes at the delta apex and TSL, including reverse flows, under various future riverbed lowering and upstream hydrology scenarios.

1D hydraulic model of the LMB

A 1D hydrodynamic model, MIKE 11, was used to simulate the hydraulics across the river network of the LMB, extending from Kratie to the delta shoreline (Fig. 1a). The model was initially set up by the Southern Institute of Water Resources Research (SIWRR) and has since been widely used to understand the hydraulics of the Lower Mekong region, notably in terms of evaluating flood risk[51,52]. Covering over 55,000 km^2, the model includes 4,235 branches, of which more than 2,134 represent floodplains. The simulated channel network extends about 25,000 km and includes 26,376 computational nodes using the WGS84 coordinate system[53]. Topographic data for the Mekong reaches in Cambodia and parts of Vietnam were sourced from 1998 surveys by the MRC (here adopted from ref. 28) and the Mekong Atlas via the MRC's ISIS model (Fig. 1a and Extended Data Fig. 2d). For small areas in the VMD lacking the 1998 bathymetry, a 1998 analogue bathymetry adopted from ref. 28 was applied (Extended Data Fig. 2d). Cross sections were extracted every ~3 km along the combined 1998 observed and estimated bathymetry surface and integrated into the 1D model. Floodplains in the Cambodian Mekong Delta, lacking major channels and dykes, were

modelled as wide cross-section channels[51]. By contrast, the VMD floodplains were segmented into flood cells to safeguard agricultural areas and were represented as wide channels bordered by weirs[51], with crest elevations modified to reflect 2000 dyke conditions[54]. The floodplain topography for both regions was based on the 2000 Shuttle Radar Topography Mission digital elevation model at 90 m resolution. The upstream model boundary was forced with daily water discharge at Kratie. Rainfall data within the Tonle Sap basin were transformed into daily discharge at 11 boundary (tributary inflow) points for the TSL by using the rainfall–run-off MIKE NAM model[51]. Rainfall and evaporation over the lake were not included in the model because, although their contributions are not synchronized, they are of comparable magnitude and are relatively small compared with the water inputs from the Tonle Sap basin tributaries and the TSR[7,9]. Downstream boundary conditions along the Mekong coast were set using observed hourly tidal water-level data from coastal stations[51] (numbers 13–22, Supplementary Table 1). Simulated water levels were output hourly and referenced to Hon Dau m.s.l., which is 0.167 m lower than Cambodia's Ha Tien m.s.l. datum[55].

Model calibration and validation

The model was calibrated using data from the extreme high-flow year of 2000, when the water volume at Kratie reached 523 km^3, considerably above the 2000–2021 average of 390 km^3 and which has an estimated 3% annual exceedance frequency within the same historical data range. Validation was performed using data from the low-flow year of 2003 (328 km^3; 72% exceedance frequency; Extended Data Fig. 3a,b). These years are representative of hydrological extremes and are close in time to the 1998 bathymetry baseline, minimizing morphological change impacts[24]. Although past errors and uncertainties exist in Kratie discharge records[56], recent analysis by Stephens[57] confirms the reliability of using data for these selected years. Discharge data from VMD gauging stations further support their representativeness (Extended Data Fig. 3a). For the Tonle Sap basin boundaries, NAM model-derived daily discharge data for 11 tributaries in 2000 and 2003 were used, with calibration for these discharges shown in Extended Data Fig. 4a–c. The total annual water volumes for these tributaries were 37.3 km^3 in 2000 and 24.3 km^3 in 2003, closely aligning with the values of 42.1 km^3 and 20.9 km^3, respectively, reported by Kummu et al.[9] (Extended Data Fig. 8). The downstream boundaries were driven by observed hourly tidal water levels along the Mekong coastal zone for 2000 and 2003, respectively. All water-level data at LMB gauging stations (Fig. 1a) were referenced to Hon Dau m.s.l. for consistent vertical alignment.

For calibration, Manning's coefficients from ref. 52 were applied and divided into three zones: main rivers, side channels and floodplains, to reflect their distinct hydraulic characteristics. Manning's n values in each zone were systematically adjusted until the optimum water level and water discharge outputs were generated (Supplementary Table 2). Model performance was assessed using the Nash–Sutcliffe coefficient (NSE; equation (1))[58]:

$$\mathrm{NSE} = 1 - \frac{\sum_{t=1}^{T}(X_{\mathrm{m}}^{t} - X_{0}^{t})^{2}}{\sum_{t=1}^{T}(X_{0}^{t} - \overline{X_{0}})^{2}} \quad (1)$$

where X_{m}^{t} is the calibrated value at time t and X_{0}^{t} is the observed data at time t; $\overline{X_{0}}$ represents the mean of observed values. NSE values below 0.5 indicate poor calibration/validation, values above 0.5 indicate satisfactory performance, values above 0.65 indicate good performance, and values exceeding 0.8 represent a highly accurate model[59].

The simulated and observed data (water level and discharge) were separated into dry and flood seasons depending on whether the daily discharge was below or above the 2000–2021 long-term average, following MRC[32] definitions, to calculate NSE values.

For the model calibration, comparisons of simulated and observed water-level series across various stations in the LMB and water discharge in the VMD (see Fig. 1a and Supplementary Table 1 for locations) are presented in Extended Data Fig. 5, while the corresponding NSE scores are presented in Supplementary Table 3. The comparisons show strong agreement between simulated and observed data for both dry and flood seasons during the test year. However, at Tan Chau station, the discharge NSE declined to 0.56, indicating satisfactory performance despite limitations, probably due to challenges in accurately modelling water exchange between the floodplain and main channel[52] during the extreme high-flow conditions of 2000. Despite these minor discrepancies, the model's performance remains reliable and effective for capturing the key hydraulic dynamics of the system.

For model validation (year 2003), the comparison between simulated and observed data is shown in Extended Data Fig. 6, while the corresponding NSE values for this analysis are provided in Supplementary Table 4. These results show that there is a robust overall agreement between the simulated outcomes and observed data across the validated year. However, the model tends to slightly overestimate water levels during the dry season in the lake system (at Kompong Luong and Prek Kdam) and at the delta apex (Chaktomuk; Extended Data Fig. 6). This dry-season overestimation in the lake probably stems from uncertainties in the simulated TSL tributary inflows, which are the sole water source during low-flow periods when the lake volume is greatly reduced, making the water in the lake more sensitive to inflow variability. At Chaktomuk, the slight overestimation may also result from modestly elevated simulated water levels in both the LMR (for example, at Kompong Cham) and the TSL.

Further validation

To validate the impact of riverbed lowering specifically on water-level reduction in the Lower Mekong system, particularly at the delta apex and during the period of historical observations, we conducted additional simulations using two bathymetry scenarios: (1) baseline historical, reflecting 1998 conditions, and (2) contemporary, reflecting 2018 conditions ('Model scenarios'). These scenarios were applied to two hydrological years: 2018 (high water flux; 454 km^3) and 2020 (low water flux; 260 km^3). Due to the absence of observed discharge data from the TSL tributaries, NAM-simulated daily inflows were used in the model scenarios for this step, these totalling 27.6 km^3 in 2018 and 16.5 km^3 in 2020 ('Model scenarios' and Extended Data Fig. 8). All other parameters remained consistent with the original calibration and validation set-up.

Supplementary Figs. 1 and 2 present comparisons of observed and simulated water levels and discharges for both bathymetry scenarios at key stations in 2018 and 2020, with Supplementary Tables 5 and 6 summarizing seasonal average results. These results indicate that, during the dry season, simulated water levels under the contemporary scenario generally correspond closely with observations across all gauges for both 2018 and 2020. During the flood season, simulated water levels under the contemporary scenario were slightly lower than observed values in the Cambodian territory (Supplementary Fig. 1 and Supplementary Tables 5 and 6). The slight underestimation of simulated flood-season water levels in Cambodia probably results from uncertainties in the contemporary bathymetry, which was not directly observed in 2018 but instead was estimated by applying an estimated riverbed lowering rate to the 1998 bathymetry dataset ('Model scenarios'). This assumption may have (1) overstated actual riverbed deepening, thereby increasing flow conveyance and lowering simulated water levels[24], and (2) overlooked localized impacts from sand mining (for example, sand pits) and sediment coarsening caused by upstream dams, factors that probably increased actual riverbed roughness and contributed to higher observed water levels[60,61], which further explains the model's underestimation. Simulated discharges generally agree with observations for both the dry and flood seasons (Supplementary Tables 5 and 6), with the exception of slight overestimations at Tan Chau and Chau Doc in Vietnam during the 2018 high-water peak (Supplementary Fig. 1), which probably results from

the underestimated water levels in the Cambodian reaches upstream, thereby reducing floodplain storage and increasing downstream flow within the river during the critical high-flood period[8,52].

A 20-year comparison of contemporary and baseline historical bathymetry scenarios reveals clear water-level decreases during both flood and dry seasons at all stations, highlighting the impact of riverbed lowering[24,47] (Supplementary Tables 5 and 6) and aligning with observed long-term trends (Supplementary Table 7). For example, averaging data from the high-flow year 2018 and low-flow year 2020, simulated water levels dropped by 1.64 m (flood season) and 1.26 m (dry season) at Chaktomuk, and by 1.39 m and 1.24 m, respectively, at Kompong Luong. Observed long-term trends support these findings. Comparing the periods 1998–2009 (midpoint 2004) and 2010–2021 (midpoint 2016), observed water levels fell by 1.38 m (flood season) and 0.42 m (dry season) at Chaktomuk and by 1.44 m and 0.70 m, respectively, at Kompong Luong (Supplementary Table 7) over the 12-year interval. However, these comparisons must be regarded as indicative because of variations in the timescales over which the data are compared.

Furthermore, recorded water levels at Stung Treng station (far upstream of the delta apex) show only a slight decline of 0.49 m during the flood season but an increase of 0.18 m during the dry season over the same period, consistent with upstream dam regulation[22] (Supplementary Table 7). By contrast, downstream stations such as Chaktomuk show more substantial declines for both the dry and flood seasons, which cannot be attributed solely to dam operations or climate variability given the relatively minor upstream changes. This discrepancy underscores the role of geomorphological changes, as the reach upstream of Kratie flows primarily over stable bedrock[6], while the downstream alluvial reaches have experienced extensive sand mining[30,62]. This has led to substantial riverbed lowering (Fig. 1a), contributing to the observed reductions in water levels[24].

For the calibration of the reverse flow volume in the TSL system, due to the absence of observed reverse discharge data, we estimated total annual reverse inflows and outflows using the baseline historical scenario (1998 bathymetry condition) under low, medium, and high water-flux conditions ('Model scenarios'). Simulated reverse inflows were around 33.2, 45.1 and 61.9 km^3, respectively, with an average of 46.7 km^3, while corresponding outflows were approximately 50, 64.7 and 89.5 km^3, averaging 69.3 km^3 (Fig. 2a–f). These estimates closely align with the average inflow of 44.3 km^3 and outflow of 71.3 km^3 reported by Kummu et al.[9] for the period 1997– 2004. In addition, modelled overland flow from the Mekong River to the lake through the TSF contributed 9.1 km^3 of floodwater to the lake during the medium-flow year, and 2.1 and 13.0 km^3 during low- and high-flux years, respectively, consistent with Fujii et al.[8], who observed a direct TSF overland flow of 11.5 km^3 during the high-flux year of 2002 (Kratie volume = 482 km^3).

Simulated reverse flow durations also align well with MRC[17] data. In the medium-flux year (2009 hydraulic condition; 'Model scenarios'), the reverse flow spans from 24 May to 15 October in the Baseline scenario (1998 bathymetry) and from 25 May to 14 October in the Contemporary scenario (2018 bathymetry), closely matching MRC[17] reported period of May 26 to October 10 for 2009. We consider the 2009 bathymetry condition to be an intermediate state between the 1998 and 2018 bathymetry conditions. Similar agreement is observed for the low-flux (2010) and high-flux (2011) years (Fig. 2d–f).

In summary, the model calibration and validation steps confirm the model's ability to capture key hydrological processes across the system. It effectively represents system-wide water levels, especially at the delta apex and TSL during the flood season, where water-level changes drive the reverse flow mechanism (as identified by MRC[7,32] and other studies[9,12,23]). It also reproduces discharge dynamics in the VMD influenced by this reversal. Importantly, the model captures the impacts of riverbed lowering on the hydraulic regime, especially water levels at the delta apex, which are critical for driving the reverse flow. The simulated reverse flow volumes and timing closely match findings from existing studies, reinforcing the model's reliability and its suitability for evaluating the effects of riverbed lowering on reverse flow dynamics.

Model scenarios

To assess the impact of riverbed lowering on the LMB hydraulics, two additional bathymetry datasets were created. The contemporary scenario (2018) was generated by updating the 1998 bathymetry with spatially observed riverbed lowering over 1998–2018. Furthermore, by assuming a persistent hypothetical trajectory of riverbed lowering at the rate observed over the 20-year period from 1998 to 2018, and anticipating the continued rates and pattern of riverbed degradation into the future[28,30], a future scenario (for year 2038) was developed. Previous studies indicate that the Tonle Sap system's morphology, including the TSL and TSR, has remained stable recently[7,13], with lake sedimentation rates of only millimetres per year[63]. Thus, both the contemporary and future bathymetry scenarios use the unchanged 1998 elevation cross-section data for the TSR and TSL. Our primary objective was to assess the impact of overall riverbed lowering rather than focusing on detailed morphological changes at individual locations. The methods for generating these scenarios are detailed in the following.

To create the contemporary bathymetry scenario for the LMR and MD distributaries, cumulative riverbed lowering from 1998 to 2018 was calculated using observed bathymetric data from 1998, 2013 and 2018 (Extended Data Fig. 2a–c). Due to data gaps covering different sections at different times, the riverbed lowering was calculated separately for each part of the system, as described in the following.

For the LMR stretch from Kratie to Neak Luong, river bathymetry digital elevation models from 1998 and 2013 (Extended Data Fig. 2a,b) were differenced using the spatial analyst toolbox (Raster Calculator) in ArcGIS. The laterally averaged depth difference was calculated at 1 km intervals along the main channel. To estimate riverbed lowering from 2013 to 2018 in this reach, several steps were undertaken. First, it was noted that sand and gravel extraction rates from Kratie to Kompong Cham were at least about ten times lower than in downstream areas[26], and minimal change was observed from 1998 to 2013. Thus, riverbed levels from Kratie to Kompong Cham were assumed unchanged between 2013 and 2018. Second, according to Hackney et al.[30], the LMR from Kompong Cham to the Cambodia–Vietnam border (Extended Data Fig. 2a,b) experienced significant riverbed lowering due to a net negative sand budget, with a median rate of 0.26 m yr^{-1} between 2013 and 2019. Thus, riverbed lowering from 2013 to 2018 was estimated at 1.3 m across this entire reach from Kompong Cham to Neak Luong. Finally, the laterally averaged depth changes from 1998 to 2013 were combined with riverbed lowering data from 2013 to 2018 to produce a continuous record of riverbed lowering at 1 km intervals along the LMR from Kratie to Neak Luong for 1998–2018.

To estimate accumulated riverbed lowering from 1998 to 2018 in the LMR stretch lacking data, from Neak Luong to the Cambodia–Vietnam border (Extended Data Fig. 2b), a linear interpolation was applied between averaged bed-lowering values at Neak Luong and the Vietnam border adopted from ref. 28 (Extended Data Fig. 2e). For the Bassac River, from the delta apex to the Vietnam border, where data are also missing, riverbed lowering was assumed equal to that of the LMR over the same reach.

The cumulative riverbed lowering data for the LMR and Bassac River in Cambodia were integrated with corresponding data from Vietnam, adopted from ref. 28 (Extended Data Fig. 2e) for the period 1998–2018. The data were initially averaged laterally at 1 km intervals, then further aggregated into 10 km segments to reduce the influence of localized sand-mining sites. The results indicate an average lowering of 3.06 m (σ = 2.03 m) across the system (Extended Data Fig. 7a).

To project future riverbed topography, it was assumed that the riverbed lowering observed from 1998 to 2018 continues beyond 2018

to 2038. This projection accounts for spatial variations in sand-layer thickness beneath the alluvial Mekong reaches, ranging 25 m south of Chaktomuk[62] to around 28 m in the MD[31], substantially exceeding the observed lowering over 1998–2018. In a small section near Kratie in the LMR, depth differences show positive values, indicating slight shallowing between 1998 and 2018 (Extended Data Fig. 7a). Accordingly, for the projected 1998–2038 depth changes, these positive values were set to 0 m, assuming no riverbed elevation change in the upper reaches of the domain over this period. This adjustment reflects the expectation that future riverbed lowering will persist due to ongoing sand mining and reduced sediment supply from upstream dams. The projected riverbed lowering from 1998 to 2038 averages 5.92 m (σ = 2.84 m) across the system (Extended Data Fig. 7a). Finally, cross sections were extracted every ~3 km along the 2018 and 2038 Mekong riverbeds and incorporated into the 1D model scenarios.

Note that our model excludes VMD dike developments as their localized impact on flood levels is minimal[54]. Given the largely unaltered Cambodian floodplain[64] and the delta apex's upstream location (~110 km from the VMD), their influence on the study area is negligible.

The three aforementioned bathymetry scenarios were simulated using upstream discharge data from 2009 2010, and 2011, which represent medium, low, and high water-flux years within the 2000–2021 period. Specifically, the year 2011 was characterized as a high-flood year, with total water volume at Kratie reaching approximately 500 km^3, corresponding to 7% annual exceedance frequency within the 2000–2021 period. The year 2009 was medium with 415 km^3 (37% exceedance), while 2010 was low at 301 km^3 (88% exceedance; Extended Data Fig. 7b,c). These hydrograph discharges represent a wide range of hydrological conditions that is sufficiently broad to encompass plausible future changes in run-off. For example, projected discharge variations at Kratie due to climate change alone (2032–2042 compared with 1982–1992) range from −11% to +15% in the flood season and −10% to +13% in the dry season. Meanwhile, dam operations are expected to moderate this variability, with flood-season flows decreasing by 5–24% and dry-season flows increasing by 25–160% (ref. 56). The simulated daily discharges at 11 Tonle Sap tributary boundaries from the NAM model were also included, with total contributions to the lake of 27.6 km^3 (2011, high flux), 22.5 km^3 (2009, medium flux) and 16.5 km^3 (2010, low flux). These values likewise reflect the hydrological variability in the Tonle Sap basin, compared with an average of 23.8 km^3 from 1997 to 2003[7] (Extended Data Fig. 8).

At the downstream boundaries, 1998 observed hourly water-level data from coastal gauges were combined with varied upstream flows, assuming constant downstream tides and neglecting sea-level rise. This yielded nine scenarios: three bathymetry conditions crossed with three upstream flow levels. The model is initialized with observed water levels from gauge stations across the LMB to ensure alignment with real-world conditions. Each scenario is simulated over a 3-year loop, using the second year for analysis.

Estimating the inundation area of TSL

The inundation area of TSL was determined using the water level–flooded area relationship from ref. 9 (equation (2)):

$$A = -5.5701 \times \mathrm{WL}^3 + 137.4 \times \mathrm{WL}^2 + 470.29 \times \mathrm{WL} + 1,680.2 \ (R^2 > 0.99) \quad (2)$$

where A is the inundation TSL area (km^2), and WL is simulated water level at Kompong Luong station (m) referenced to Ha Tien m.s.l.

The long-term average flooded area (A_f) was calculated by averaging the inundated areas estimated from observed daily water levels at Kompong Luong over the period from 1998 to 2021.

We assume that the rating curves used, based on 1997–2005 data[9], remain applicable due to minimal recent geomorphological changes in the lake[13,63].

Reporting summary

Further information on research design is available in the Nature Portfolio Reporting Summary linked to this article.

Data availability

The 2018 riverbed bathymetry data used in this study were obtained from ref. 28 and are publicly available at https://hydra.hull.ac.uk/resources/hull:17951. The 2013 riverbed bathymetry data were obtained from ref. 30 and are available on request from the corresponding author of that study (christopher.hackney@newcastle.ac.uk). Hydrological data for gauging stations in Cambodia are available through the Mekong River Commission Data Portal at https://portal.mrcmekong.org/monitoring/river-monitoring-telemetry. Hydrological data for gauging stations in Vietnam can be requested from the Southern Regional Hydro-Meteorological Centre (SRHMC, at http://www.kttv-nb.org.vn/), Vietnam. The 1D model of the Lower Mekong Basin can be requested from the Southern Institute of Water Resources Research (SIWRR, at http://www.siwrr.org.vn/?lang=e), Vietnam.

References

1. Bonheur, N. & Lane, D. B. Natural resources management for human security in Cambodia's Tonle Sap biosphere reserve. *Environ. Sci. Policy* **5**, 33–41 (2002).
2. *Promoting Conservation at Tonle Sap Biosphere Reserve* (UNESCO, 2023); https://www.unesco.org/en/articles/promoting-environmental-conservation-tonle-sap-biosphere-reserve
3. Campbell, I. C., Poole, C., Giesen, W. & Valbo-jorgensen, J. Species diversity and ecology of Tonle Sap Great Lake, Cambodia. *Aquat. Sci.* **68**, 355–373 (2006).
4. Arias, M. E., Cochrane, T. & Elliott, V. Modelling future changes of habitat and fauna of the Tonle Sap wetland of the Mekong. *Environ. Conserv.* **41**, 165–175 (2014).
5. Kingston, D. G., Thompson, J. R. & Kite, G. Uncertainty in climate change projections of discharge for the Mekong River Basin. *Hydrol. Earth Syst. Sci.* **15**, 1459–1471 (2011).
6. *Overview of the Hydrology of the Mekong Basin* (MRC, 2005).
7. *Final Report—Part 2: Research Findings and Recommendations. WUP-FIN Phase 2—Hydrological, Environmental and Socio-Economic Modelling Tools for the Lower Mekong Basin Impact Assessment* (MRCS/WUP-FIN, 2007).
8. Fujii, H. et al. Hydrological roles of the Cambodian floodplain of the Mekong River. *Int. J. River Basin Manage.* **1**, 253–266 (2003).
9. Kummu, M. et al. Water balance analysis for the Tonle Sap Lake–floodplain system. *Hydrol. Process.* **28**, 1722–1733 (2014).
10. Xu, Z. et al. Morphological characteristics of Cambodia Mekong Delta and Tonle Sap Lake and its response to river–lake water exchange pattern. *J. Water Resour. Prot.* **12**, 275–302 (2020).
11. Cochrane, T. A., Arias, M. E. & Piman, T. Historical impact of water infrastructure on water levels of the Mekong River and the Tonle Sap system. *Hydrol. Earth Syst. Sci.* **18**, 4529–4541 (2014).
12. Arias, M. E., Piman, T., Lauri, H., Cochrane, T. A. & Kummu, M. Dams on Mekong tributaries as significant contributors of hydrological alterations to the Tonle Sap Floodplain in Cambodia. *Hydrol. Earth Syst. Sci.* **18**, 5303–5315 (2014).
13. NG, W. X. & Park, E. Shrinking Tonlé Sap and the recent intensification of sand mining in the Cambodian Mekong River. *Sci. Total Environ.* **777**, 146180 (2021).
14. Chua, S. D. X., Lu, X. X., Oeurng, C., Sok, T. & Grundy-Warr, C. Drastic decline of flood pulse in the Cambodian floodplains (Mekong River and Tonle Sap system). *Hydrol. Earth Syst. Sci.* **26**, 609–625 (2022).
15. Dang, H. et al. Hydrologic balance and inundation dynamics of Southeast Asia's largest inland lake altered by hydropower dams in the Mekong River basin. *Sci. Total Environ.* **831**, 154833 (2022).

16. Morovati, K. et al. Contributions from climate variation and human activities to flow regime change of Tonle Sap Lake from 2001 to 2020. *J. Hydrol.* **616**, 128800 (2023).
17. *Article 6B for Monitoring Purposes* (MRC, accessed25 January 2025); https://pmfm.mrcmekong.org/monitoring/6b/
18. Frappart, F. et al. Influence of recent climatic events on the surface water storage of the Tonle Sap Lake. *Sci. Total Environ.* **636**, 1520–1533 (2018).
19. Wang, Y., Feng, L., Liu, J., Hou, X. & Chen, D. Changes of inundation area and water turbidity of Tonle Sap Lake: responses to climate changes or upstream dam construction?. *Environ. Res. Lett.* **15**, 0940a1 (2020).
20. Kummu, M. & Sarkkula, J. Impact of the Mekong River flow alteration on the Tonle Sap flood pulse. *Ambio* **37**, 185–192 (2008).
21. Huang, W., Park, E., Wang, J. & Sophal, T. The changing rainfall patterns drive the growing flood occurrence in Phnom Penh, Cambodia. *J. Hydrol. Reg. Stud.* **55**, 101945 (2024).
22. Räsänen, T. A. et al. Observed river discharge changes due to hydropower operations in the Upper Mekong Basin. *J. Hydrol.* **545**, 28–41 (2017).
23. Ji, X. & Li, Y. Changes in the lake area of Tonle Sap: possible linkage to runoff alterations in the Lancang River? *Remote Sens.* **10**, 866 (2018).
24. Chua, S. D. & Lu, X. X. What can stage curves tell us about water level changes? Case study of the Lower Mekong Basin. *Catena* **216**, 106385 (2022).
25. *Greater Mekong. Dams in the Mekong River Basin: Commissioned, Under Construction and Planned Dams in April 2016. Vientiane, CGIAR Research Program on Water, Land and Ecosystems—Greater Mekong* (WLE, 2016).
26. Bravard, J. P., Goichot, M. & Gaillot, S. Geography of sand and gravel mining in the Lower Mekong River. *EchoGéo* **26**, 1–20 (2013).
27. Brunier, G., Anthony, E. J., Goichot, M., Provansal, M. & Dussouillez, P. Recent morphological changes in the Mekong and Bassac river channels, Mekong Delta: The marked impact of river-bed mining and implications for delta destabilisation. *Geomorphology* **224**, 177–191 (2014).
28. Vasilopoulos, G. et al. Establishing sustainable sediment budgets is critical for climate-resilient mega-deltas. *Environ. Res. Lett.* **16**, 064089 (2021).
29. Gruel, C. R. et al. New systematically measured sand mining budget for the Mekong Delta reveals rising trends and significant volume underestimations. *Int. J. Appl. Earth Obs. Geoinf.* **108**, 102736 (2022).
30. Hackney, C. R. et al. Sand mining far outpaces natural supply in a large alluvial river. *Earth Surf. Dyn.* **9**, 1323–1334 (2021).
31. Hackney, C. R. et al. River bank instability from unsustainable sand mining in the lower Mekong River. *Nat. Sustain.* **3**, 217–225 (2020).
32. *State of the Basin Report* (MRC, 2018).
33. Baran, E. Mekong fisheries and mainstream dams. In *Mekong River Commission Strategic Environmental Assessment of Hydropower on the Mekong Mainstream*, 1–145 (International Centre for Environmental Management, 2010).
34. Chevalier, M. et al. Long-term data show alarming decline of majority of fish species in a Lower Mekong basin fishery. *Sci. Total Environ.* **891**, 164624 (2023).
35. Zalinge, N., Nao, T. & Touch, S. T. *Where There Is Water, There Is Fish? Fisheries Issues in the Lower Mekong Basin from a Cambodian Perspective* (MRC/Dof/Danida, 1998).
36. Sok, T. et al. Nutrient transport and exchange between the Mekong River and Tonle Sap Lake in Cambodia. *Ecol. Eng.* **176**, 106527 (2022).
37. Lohani, S., Dilts, T. E., Weisberg, P. J., Null, S. E. & Hogan, Z. S. Rapidly accelerating deforestation in Cambodia's Mekong River basin: a comparative analysis of spatial patterns and drivers. *Water* **12**, 2191 (2020).
38. Eslami, S. et al. Dynamics of salt intrusion in the Mekong Delta: results of field observations and integrated coastal–inland modelling. *Earth Surf. Dyn.* **9**, 953–976 (2021).
39. Kondolf, G. M. et al. Sustainable sediment management in reservoirs and regulated rivers: experiences from five continents. *Earths Future*. **2**, 256–280 (2014).
40. Lai, Y. G., Huang, J. & Greimann, B. P. Hydraulic flushing of sediment in reservoirs: best practices of numerical modeling. *Fluids* **9**, 38 (2024).
41. Hu, P., Cao, Z., Pender, G. & Tan, G. Numerical modelling of turbidity currents in the Xiaolangdi reservoir, Yellow River, China. *J. Hydrol.* **464–465**, 41–53 (2012).
42. Bendixen, M., Best, J. L., Hackney, C. & Iversen, L. L. Time is running out for sand. *Nature* **571**, 29–31 (2019).
43. Best, J. Anthropogenic stresses on the world's big rivers. *Nat. Geosci.* **12**, 7–21 (2019).
44. Hackney, C. R. Migrating sands: refocusing transboundary flows from water to sediment. *Area* **57**, e12954 (2024).
45. Lane, S. N. Hydraulic modelling in hydrology and geomoprhology: a review of high resolution approaches. *Hydrol. Process.* **12**, 1131–1150 (1998).
46. Twigt, D. J., De Goede, E. D., Zijl, F., Schwanenberg, D. & Chiu, A. Y. W. Coupled 1D–3D hydrodynamic modelling, with application to the Pearl River Delta. *Ocean Dyn.* **59**, 1077–1093 (2009).
47. Bao, S. et al. Peak water level response to channel deepening depends on interaction between tides and the river flow. *J. Geophys. Res. Oceans* **127**, e2021JC017625 (2022).
48. Ralston, D. K., Talke, S., Geyer, W. R., Al-Zubaidi, H. A. M. & Sommerfield, C. K. Bigger tides, less flooding: effects of dredging on barotropic dynamics in a highly modified estuary. *J. Geophys. Res. Oceans* **124**, 196–211 (2019).
49. Binh, D. V. et al. Effects of riverbed incision on the hydrology of the Vietnamese Mekong Delta. *Hydrol. Process.* **35**, e14030 (2021).
50. Yao, J., Zhang, D., Li, Y., Zhang, Q. & Gao, J. Quantifying the hydrodynamic impacts of cumulative sand mining on a large river-connected floodplain lake: Poyang Lake. *J. Hydrol.* **579**, 124156 (2019).
51. Dung, N. V. Multi-objective Automatic Calibration of Hydrodynamic mModels—Development of the Concept and an Application in the Mekong Delta. PhD thesis, Univ. Stuttgart (2011); http://elib.uni-stuttgart.de/opus/volltexte/2012/6831/
52. Manh, N. V., Dung, N. V., Hung, N. N., Merz, B. & Apel, H. Large-scale suspended sediment transport and sediment deposition in the Mekong Delta. *Hydrol. Earth Syst. Sci.* **18**, 3033–3053 (2014).
53. Dung, N. V., Merz, B., Bárdossy, A., Thang, T. D. & Apel, H. Multi-objective automatic calibration of hydrodynamic models utilizing inundation maps and gauge data. *Hydrol. Earth Syst. Sci.* **15**, 1339–1354 (2011).
54. Triet, N. V. K. et al. Has dyke development in the Vietnamese Mekong Delta shifted flood hazard downstream? *Hydrol. Earth Syst. Sci. Discuss.* **21**, 3991–4010 (2017).
55. *TCVN 8478:2010_Hydraulic Work—Demand for Element and Volume of the Topographic Survey in Design Stages, Ministry of Science and Technology, Hanoi, Vietnam* (Ministry of Science and Technology, 2010).
56. Lauri, H. et al. Future changes in Mekong River hydrology: impact of climate change and reservoir operation on discharge. *Hydrol. Earth Syst. Sci.* **16**, 4603–4619 (2012).

57. Stephens, J. A. A Critical Evaluation of Science-Generated Myths of the Mekong River Basin: Evidence-Based Analyses of Data Reliability and the Plausibility of Reported Findings (1924–2021). PhD thesis, Univ. Exeter (2023).
58. Nash, J. E. & Sutcliffe, J. V. River flow forecasting through conceptual models part I—a discussion of principles. *J. Hydrol.* **10**, 282–290 (1970).
59. Ritter, A. & Muñoz-carpena, R. Performance evaluation of hydrological models: statistical significance for reducing subjectivity in goodness-of-fit assessments. *J. Hydrol.* **480**, 33–45 (2013).
60. Hackney, C. R. et al. Increased hydraulic roughness in alluvial rivers created by sand-mining sculpted bed features. *J. Geophys. Res. Earth Surf.* **130**, e2024JF008189 (2025).
61. Chai, Y. et al. Evolution characteristics and driving factors of the water level at the same discharge in the Jingjiang reach of Yangtze River. *J. Geogr. Sci.* **30**, 1633–1648 (2020).
62. Uhlemann, S., Kuras, O., Richards, L. A., Naden, E. & Polya, D. A. Electrical resistivity tomography determines the spatial distribution of clay layer thickness and aquifer vulnerability, Kandal Province, Cambodia. *J. Asian Earth Sci.* **147**, 402–414 (2017).
63. Penny, D., Cook, G. & Sok, S. I. Long-term rates of sediment accumulation in the Tonle Sap, Cambodia: a threat to ecosystem health?. *J. Paleolimnol.* **33**, 95–103 (2005).
64. Horton, A. J. et al. The Cambodian Mekong floodplain under future development plans and climate change. *Nat. Hazards Earth Syst. Sci.* **22**, 967–983 (2022).

Acknowledgements

This work was supported by the Energy and Environment Institute, University of Hull, through a funded PhD scholarship, and by the Geography and Environment Department at Loughborough University, UK (L.Q.Q.). Additional funding support was provided through a NUACT Fellowship from Newcastle University (C.R.H.); the UK Natural Environmental Research Council (NERC) via project numbers NE/P014704/1 (to D.R.P. and S.E.D) and NE/S003150/1 (to S.E.D); the European Research Council (ERC) under the European Union's Horizon 2020 Research and Innovation programme (GEOSTICK, grant agreement 725955, D.R.P.). L.Q.Q also thanks the Southern Institute of Water Resources Research (SIWRR; N. Viet Dung) and the Ministry of Science and Technology in Vietnam (NAFOSTED-RUCK, project number NE/S003150/1) for the support on model set-up.

Author contributions

L.Q.Q., C.R.H., G.V., S.E.D. and D.R.P. conceptualized the study. L.Q.Q., C.R.H., G.V., T.C., S.E.D. and D.R.P. developed the methodology. C.R.H., G.V., N.N.H., S.E.D. and D.R.P. provided resources. L.Q.Q. conducted the formal analysis and investigation. C.R.H., G.V., T.C. and D.R.P. supervised the work. D.R.P. and S.E.D. secured funding. L.Q.Q. created the visualizations. L.Q.Q. prepared the original draft with contributions from S.E.D. and D.R.P. All authors participated in the review and editing of the paper.

Competing interests

The authors declare no competing interests.

Additional information

Extended data is available for this paper at https://doi.org/10.1038/s41893-025-01677-8.

Supplementary information The online version contains supplementary material available at https://doi.org/10.1038/s41893-025-01677-8.

Correspondence and requests for materials should be addressed to L. Q. Quan.

Peer review information *Nature Sustainability* thanks Marc Goichot and the other, anonymous, reviewer(s) for their contribution to the peer review of this work.

https://doi.org/10.1038/s41893-025-01677-8

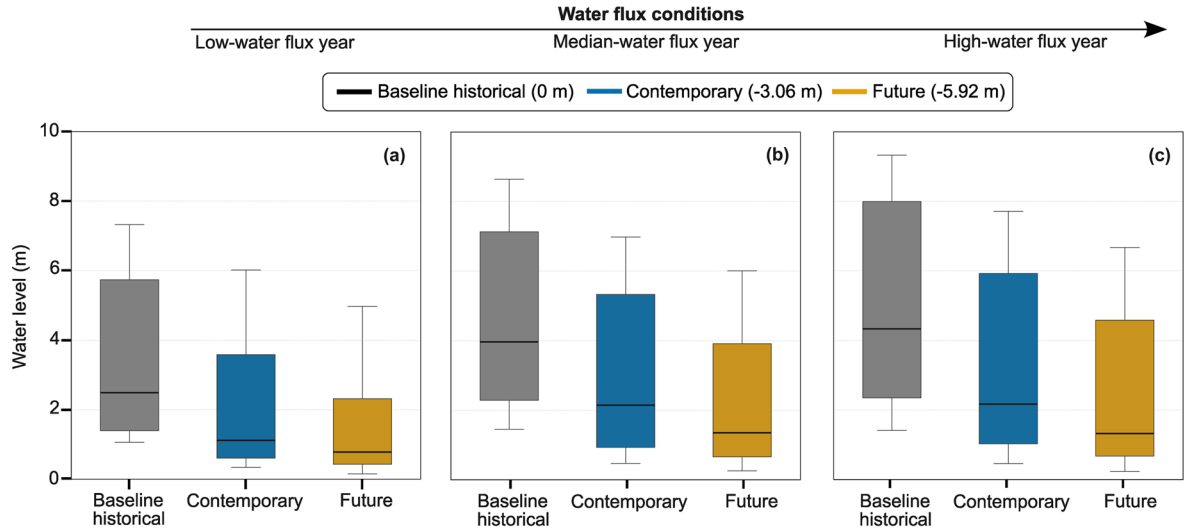

Extended Data Fig. 1 | Hydrological impacts of riverbed lowering on water level at the delta apex. (**a**–**c**) Box plots depicting the daily simulated water levels at the delta apex (Chaktomuk gauge, referenced to Hon Dau msl; n = 365 daily simulated water levels) over a one-year simulation period for the Baseline historical, Contemporary, and projected Future bathymetries under three different hydrograph flux conditions. In each box plot the central line represents the median daily water level, the box bounds indicate the 25th–75th percentiles (with 25% and 75% of daily water levels falling below these values, respectively), and the whiskers show the full range of simulated daily water levels (minimum to maximum).

https://doi.org/10.1038/s41893-025-01677-8

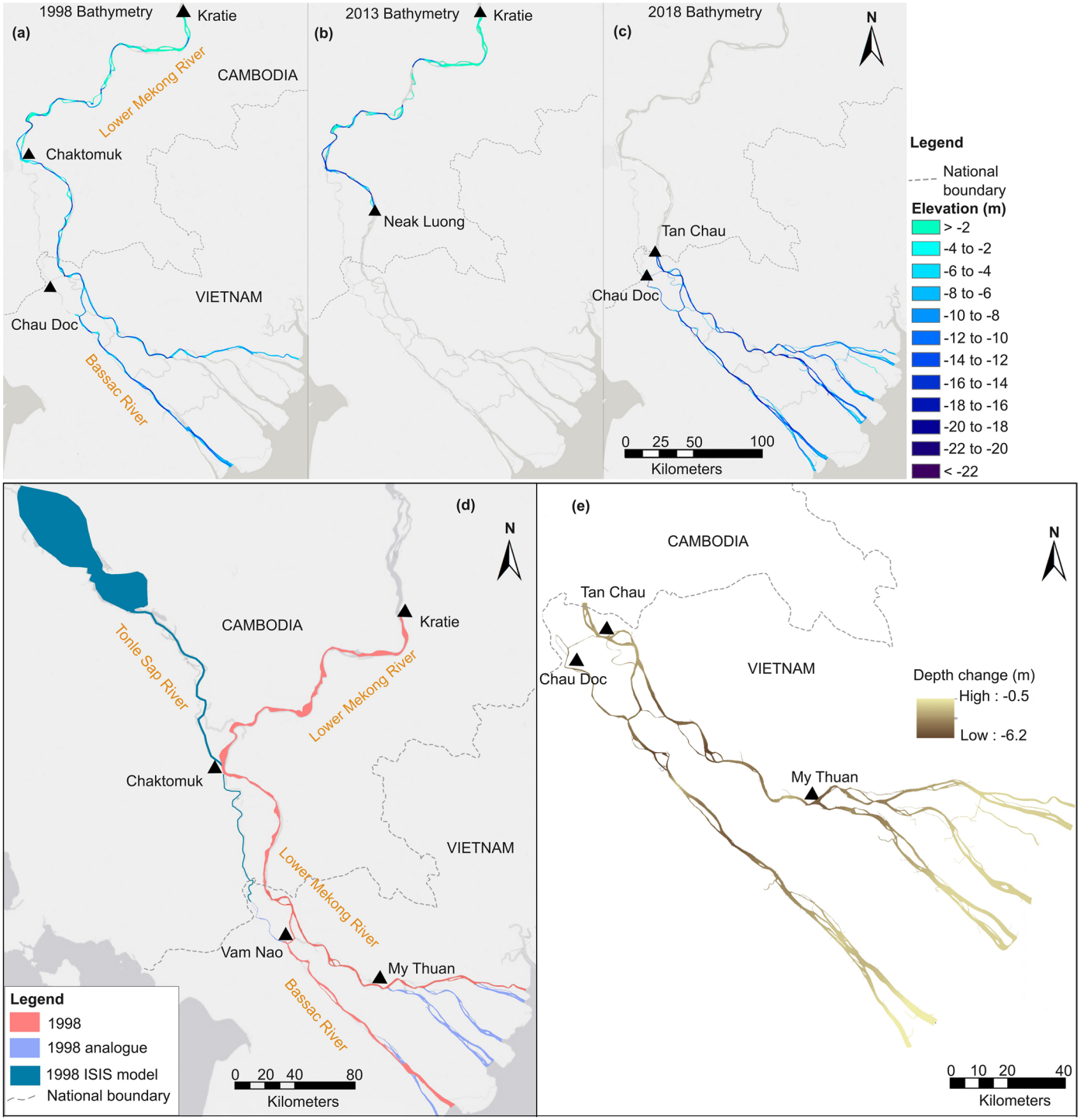

Extended Data Fig. 2 | Bathymetry datasets for 1D modelling. (**a**) The 1998 bathymetric dataset collected for the Lower Mekong River (LMR) during the 1998 survey by the Mekong River Commission (MRC) (www.mrcmekong.org). This dataset comprises a series of riverbed elevation points that cover a significant portion of the main Mekong channel in the Cambodia region, but they only cover approximately 51% of the principal distributary channels within the VMD. These bathymetric records were obtained from Vasilopoulos et al.[28]; (**b**) The bathymetric data for the year 2013 was collected from Hackney et al.[30], with a primary focus on the main LMR from Kratie to Neak Luong in Cambodia; (**c**) The river bathymetry dataset for 2018 exclusively covers territory in Vietnam, extending from Tan Chau in the LMR and Chau Doc in the Bassac River to the Mekong coastal zone, and was obtained from Vasilopoulos et al.[28]. These three bathymetric datasets are referenced to the WGS84 coordinates and Hon Dau vertical datum. Then, these bathymetric datasets are transformed into elevation surface maps (DEMs), using ArcGIS version 10.8 software. This transformation is accomplished through the application of the kriging interpolation toolkit, resulting in an interpolated grid resolution of 50 m; (**d**) The coverage areas of the different mainstream river bathymetry datasets employed in generating a cross-sectional dataset for 1D modelling; (**e**) The spatial progression of main channels deepening in VMD from 1998 to 2018 as adopted from Vasilopoulos et al.[28]. Credit: basemaps, Esri, USGS | Esri, TomTom, FAO, NOAA, USGS.

https://doi.org/10.1038/s41893-025-01677-8

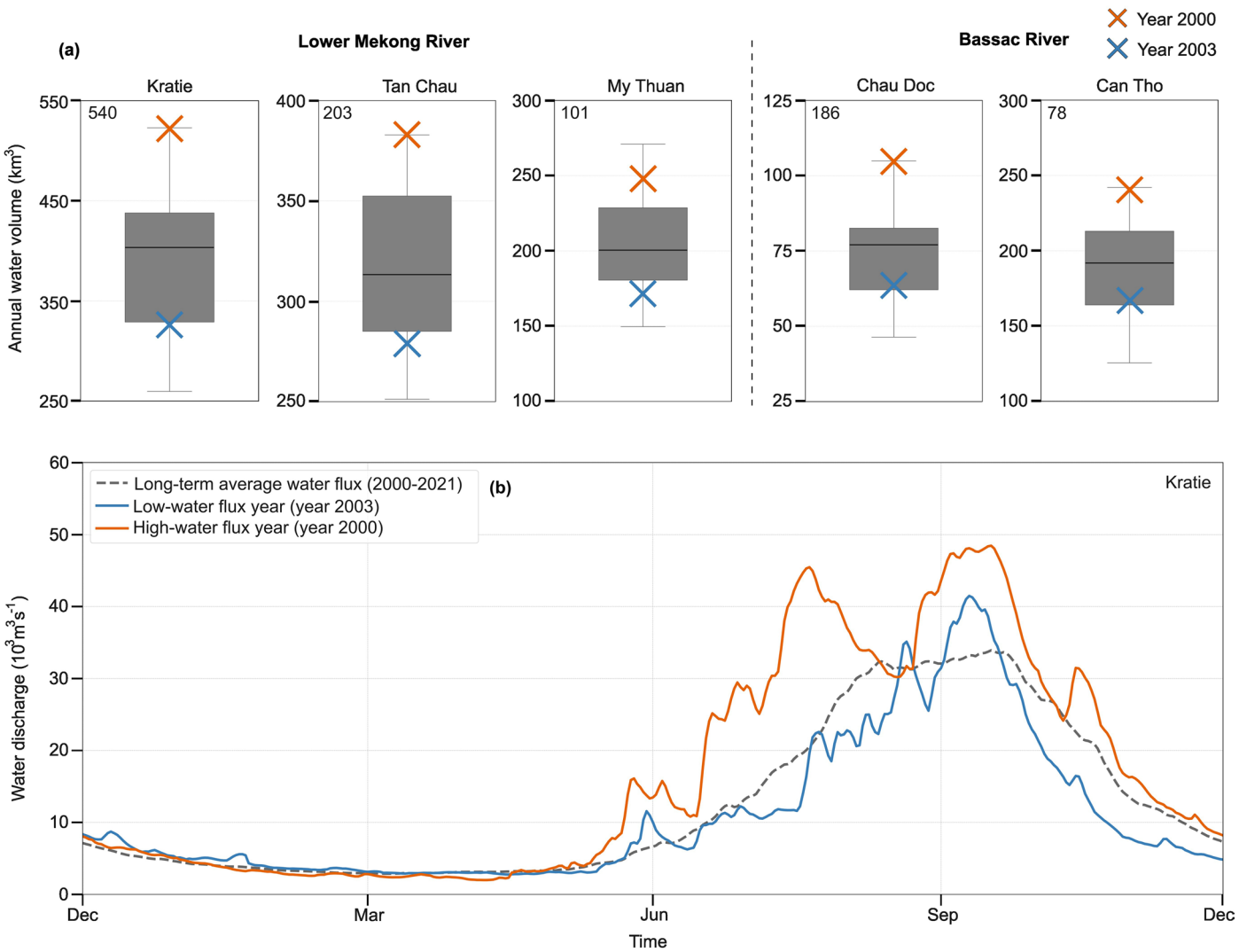

Extended Data Fig. 3 | Observed annual flow volumes in the Lower Mekong (2000–2021) and selected years for model calibration and validation. (**a**) Box plots showing the range of observed annual flow volumes at selected monitoring gauges within the lower Mekong system as measured from MRC and the Southern Regional Hydro-Meteorological Centre, Vietnam (SRHMC) for 2000-2021 (n = 22 annual water volume values per gauge), highlighting the distinct years chosen to simulate high (2000) and low (2003) flow discharge conditions in order to calibrate and validate the numerical model. In each box plot, the central line represents the median annual water volume, the box bounds indicate the 25th–75th percentiles, with 25% and 75% of annual volumes falling below these values, and the whiskers show the full range of observed annual water volumes (minimum to maximum). The number stated at the upper left corner of each panel specifies the distance from the gauge to the channel mouth; (**b**) Observed long-term average hydrograph for Kratie for 2000-2021 (black) also showing hydrographs for 2000 (orange) and 2003 (blue) as used in model calibration and validation.

https://doi.org/10.1038/s41893-025-01677-8

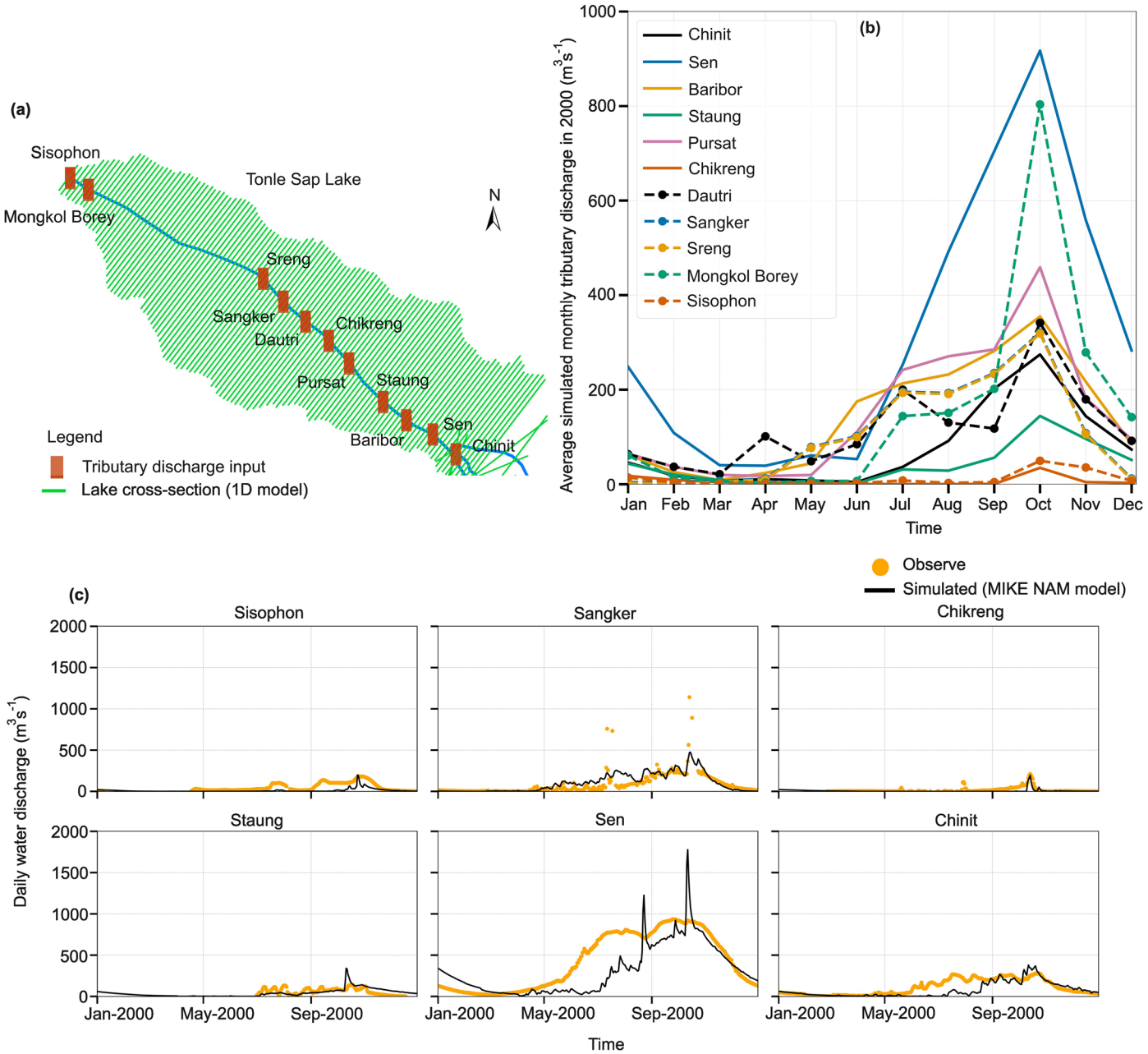

Extended Data Fig. 4 | Tonle Sap Lake tributary discharges used in the 1D model. (**a**) Tributary discharge inputs used in the 1D model; (**b**) Average simulated monthly discharge of Tonle Sap tributaries for the year 2000, extracted from the MIKE NAM model, which is consistent with the 1997–2005 average monthly discharge of Tonle Sap tributaries reported in Fig. 3b of Kummu et al.[9]; (**c**) Comparison between observed and simulated discharge in Tonle Sap Basin tributaries for the year 2000.

https://doi.org/10.1038/s41893-025-01677-8

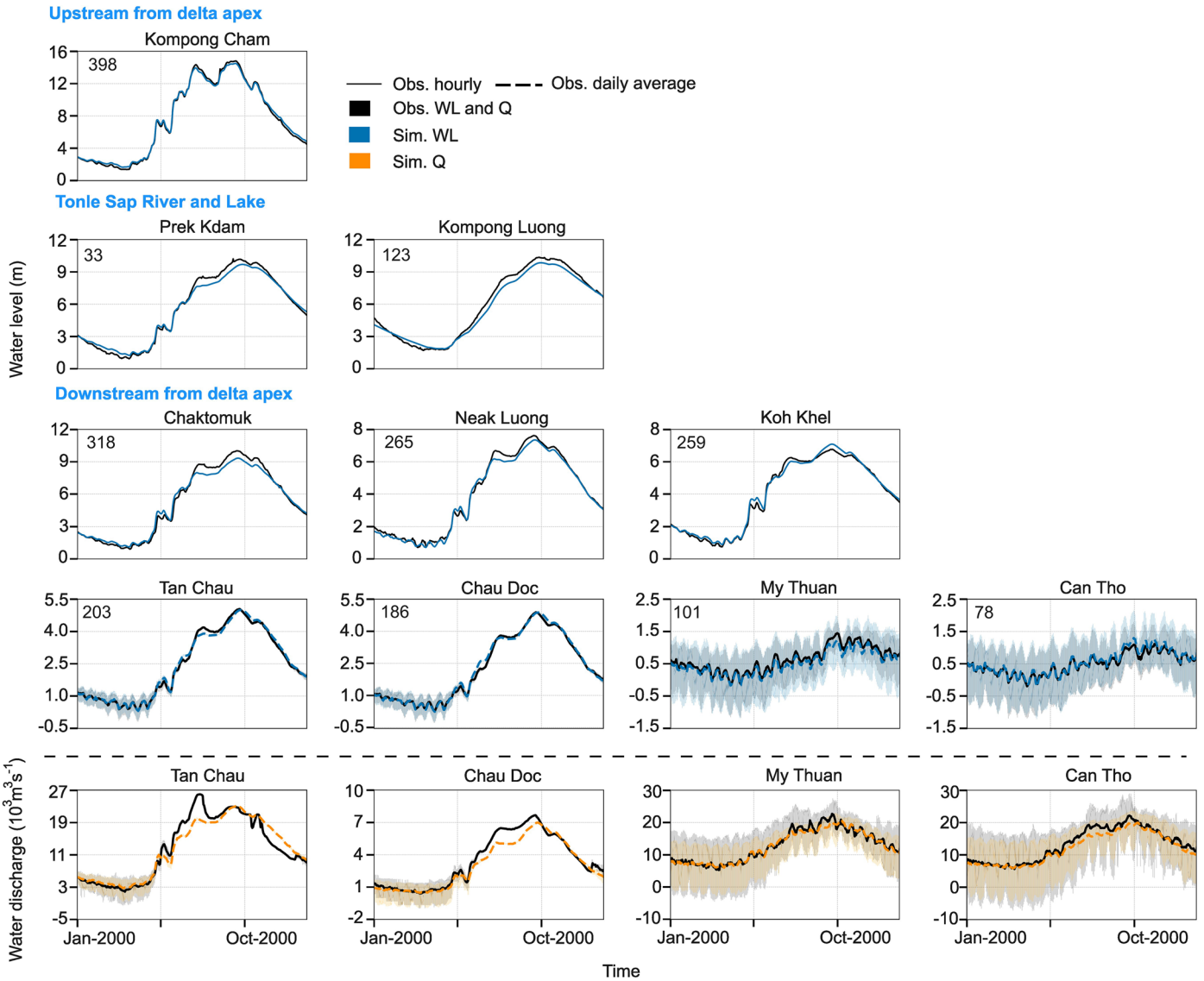

Extended Data Fig. 5 | 1D model hydraulic calibration: water levels and discharges. Assessing the agreement between the predicted and observed data for water levels (referenced to Hon Dau msl) and water discharges at monitoring stations located throughout the lower Mekong system during the calibration run for the high-water flux year of 2000 (starting from February to end of December, due to missing discharge data at Kratie). The number stated at the upper left corner of each panel typically specifies the distance from the gauge to the channel mouth, however for Prek Kdam and Kompong Luong on the TSR and TSL, the stated values represent the distance from the gauges to the delta apex. The upstream stations within Cambodia's territory (Kompong Cham, Prek Kdam, Kompong Luong, Chaktomuk, Neak Luong and Koh Khel) only provide water level data at a daily resolution, therefore the simulated data in these areas is also organized into daily data for purposes of comparison. In contrast, the values in the VMD encompass both water level and water discharge data at hourly intervals. This hourly data allows for the visualization of tidal amplitudes through subtle colour variations. Additionally, organizing this data into daily increments, as demonstrated for the upstream gauges, allows for the presentation of the overarching trends in water level or water discharge.

https://doi.org/10.1038/s41893-025-01677-8

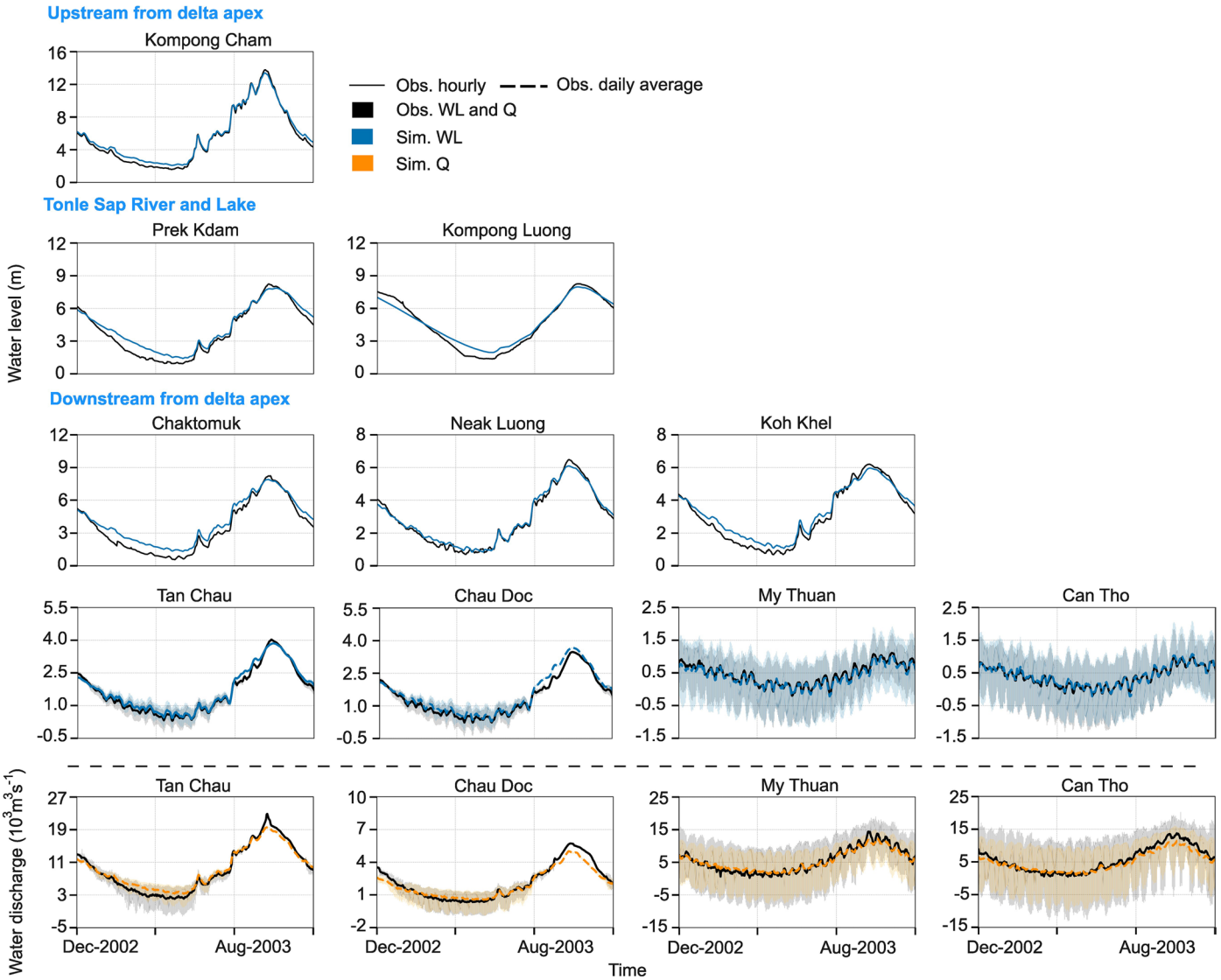

Extended Data Fig. 6 | 1D model hydraulic validation: water Levels and discharges. Comparison of simulated and observed water levels and water discharges at selected monitoring stations located across the lower Mekong system during the validation run for the low-water flux year of 2003 (December 2002-November 2003).

https://doi.org/10.1038/s41893-025-01677-8

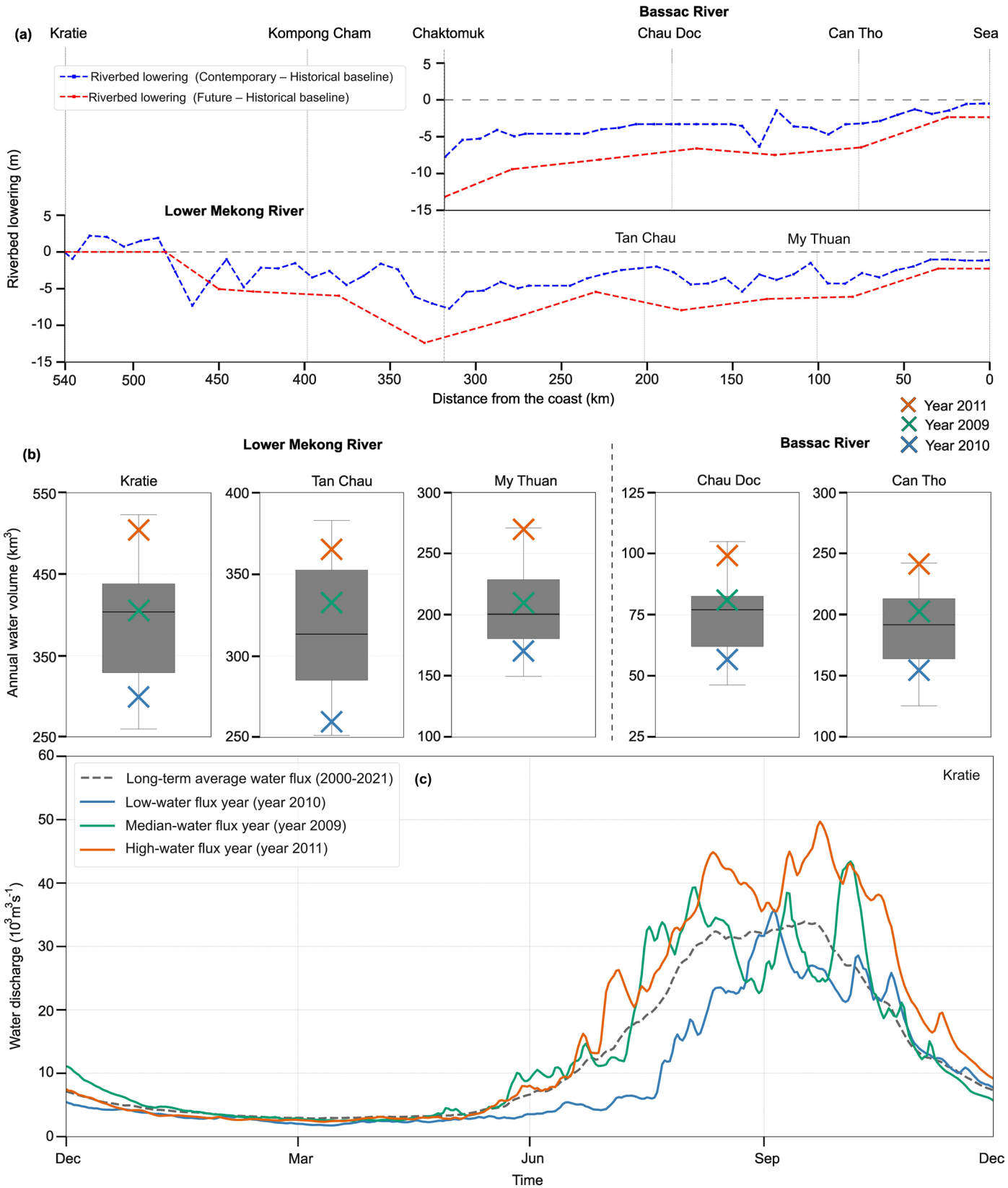

Extended Data Fig. 7 | Riverbed lowering and upstream hydrograph model scenarios. (**a**) Development of two scenarios for the accumulated average riverbed lowering between 1998-2018 and 1998-projected 2038 along the longitudinal axis of the two main Lower Mekong and Bassac Rivers. The outcomes show an average riverbed lowering of 3.06 m (σ = 2.03 m) from 1998 to 2018 and 5.92 m (σ = 2.84 m) for the 1998 to 2038 scenarios for both channels; (**b**) Boxplots of total annual water volume recorded at different gauges across the lower Mekong system for the 2000-2021 period (n = 22 annual water volume values per gauge) highlighting datasets for the high- (2011) medium- (2009) and low-(2010) water flux years. In each box plot, the central line represents the medium annual water volume, the box bounds indicate the 25th–75th percentiles, with 25% and 75% of annual volumes falling below these values, and the whiskers show the full range of observed annual water volumes (minimum to maximum); (**c**) Discharge hydrographs as estimated at Kratie for the years 2011 (high flow scenario), 2009 (medium flow scenario), and 2010 (low flow scenario) in relation to the long term mean hydrograph for the period 2000-2021.

https://doi.org/10.1038/s41893-025-01677-8

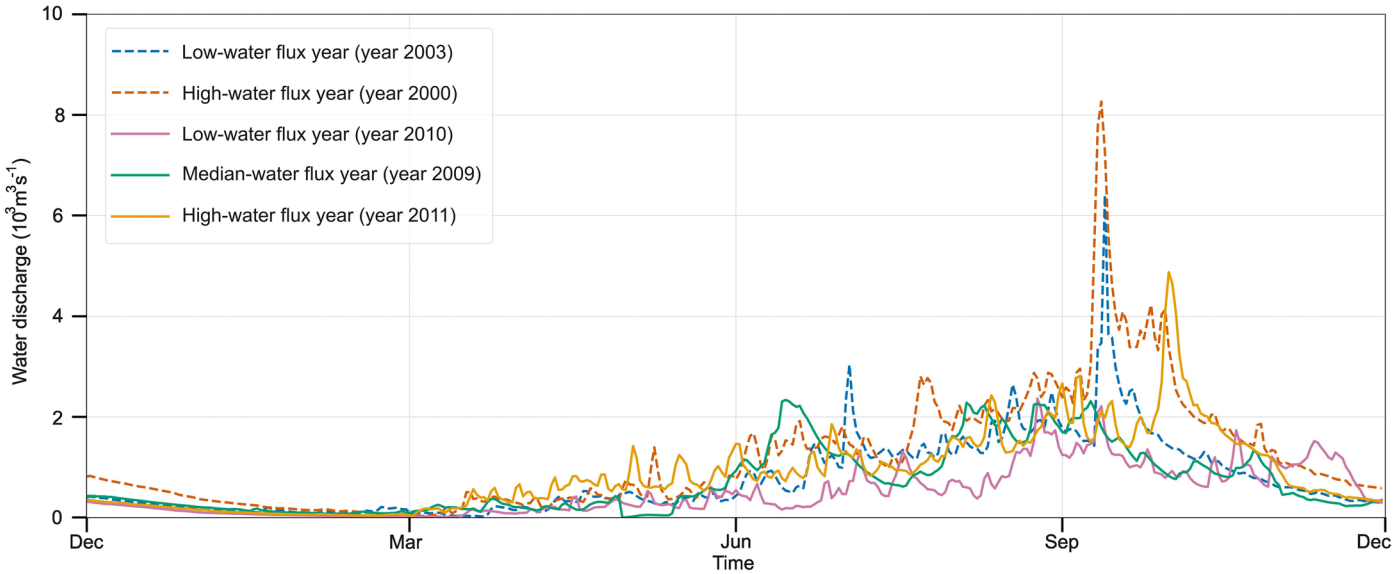

Extended Data Fig. 8 | Tonle Sap Lake tributary discharges for model calibration, validation, and scenarios. Hydrographs of total water discharge across 11 tributaries in the Tonle Sap Basin, estimated during the calibration and validation steps for the year 2000 (high-flow) and 2003 (low-flow), as well as for model scenarios in 2011 (high-flow), 2009 (medium-flow) and 2010 (low-flow).

https://doi.org/10.1038/s41893-025-01677-8

Extended Data Table 1 | Hydrological impacts of riverbed lowering on Tonle Sap reverse flow (corresponding to Fig. 2a–f)

	Total flow (km^3)			Maximum discharges (m^3s^{-1})			Duration (days)		
	Base.	Con.	Future	Base.	Con.	Future	Base.	Con.	Future
Low. flux	33.2	16.7 (-49.7%)	9.1 (-72.6%)	8,147	4,911 (-39.7%)	3,422 (-58.0%)	128	82 (-35.9%)	72 (-43.8%)
Median. flux	45.1	24.0 (-46.8%)	13.9 (-69.2%)	9,084	5,390 (-40.7%)	3,675 (-59.5%)	136	121 (-11.0%)	91 (-33.1%)
High. flux	61.9	37.1 (-40.1%)	22.4 (-63.8%)	11,539	6,965 (-39.6%)	4,668 (-59.5%)	139	114 (-18.0%)	107 (-23.0%)

Total water volume, maximum discharge, and reverse flow duration from the LMR to the TSL at Prek Kdam, under the Baseline historical (Base.), Contemporary (Con.), and Future riverbed bathymetries across various upstream hydrograph conditions. Percentages in parentheses show changes relative to the Baseline historical scenarios, with negative values indicating reductions.

https://doi.org/10.1038/s41893-025-01677-8

Extended Data Table 2 | Hydrological impacts of riverbed lowering on Tonle Sap water level and inundation (corresponding to Fig. 3a–i)

	Maximum water level (m)			Maximum flooded area (km^2)			Extended duration of A_f (days)		
	Base.	Con.	Future	Base.	Con.	Future	Base.	Con.	Future
Low. flux	7.20	5.42 (1.78)	4.3 (2.90)	10,375	7,621 (2,754)	6,027 (4,348)	156	86 (70)	0 (156)
Median. flux	8.63	6.66 (1.97)	5.42 (3.21)	12,653	9,525 (3,128)	7,624 (5,029)	213	148 (65)	99 (114)
High. flux	9.92	7.96 (1.96)	6.63 (3.29)	14,690	11,585 (3,105)	9,482 (5,208)	236	178 (58)	141 (95)

The maximum water level, maximum flooded area, and extended duration of the long-term average flooded Area; A_i in the Tonle Sap Lake for the Baseline historical (Base.), Contemporary (Con.), and Future riverbed scenarios, across the various upstream forcing hydrograph conditions. The simulated reductions for each scenario compared to the Baseline historical scenario are shown in parentheses.

nature portfolio

Corresponding author(s): Quan Quan Le

Last updated by author(s): 2025-9-17

Reporting Summary

Nature Portfolio wishes to improve the reproducibility of the work that we publish. This form provides structure for consistency and transparency in reporting. For further information on Nature Portfolio policies, see our Editorial Policies and the Editorial Policy Checklist.

Statistics

For all statistical analyses, confirm that the following items are present in the figure legend, table legend, main text, or Methods section.

n/a	Confirmed
☐	☒ The exact sample size (*n*) for each experimental group/condition, given as a discrete number and unit of measurement
☒	☐ A statement on whether measurements were taken from distinct samples or whether the same sample was measured repeatedly
☒	☐ The statistical test(s) used AND whether they are one- or two-sided *Only common tests should be described solely by name; describe more complex techniques in the Methods section.*
☒	☐ A description of all covariates tested
☒	☐ A description of any assumptions or corrections, such as tests of normality and adjustment for multiple comparisons
☒	☐ A full description of the statistical parameters including central tendency (e.g. means) or other basic estimates (e.g. regression coefficient) AND variation (e.g. standard deviation) or associated estimates of uncertainty (e.g. confidence intervals)
☒	☐ For null hypothesis testing, the test statistic (e.g. *F*, *t*, *r*) with confidence intervals, effect sizes, degrees of freedom and *P* value noted *Give P values as exact values whenever suitable.*
☒	☐ For Bayesian analysis, information on the choice of priors and Markov chain Monte Carlo settings
☒	☐ For hierarchical and complex designs, identification of the appropriate level for tests and full reporting of outcomes
☒	☐ Estimates of effect sizes (e.g. Cohen's *d*, Pearson's *r*), indicating how they were calculated

Our web collection on statistics for biologists contains articles on many of the points above.

Software and code

Policy information about availability of computer code

Data collection	No software was used for data collection
Data analysis	River bathymetry was processed with the Spatial Analyst toolbox (Raster Calculator) in ArcGIS version 10.8 . Water level and discharge data were analyzed using Python (v3.10), and figures were visualized using Python (v3.10), ArcGIS Pro, and Inkscape

For manuscripts utilizing custom algorithms or software that are central to the research but not yet described in published literature, software must be made available to editors and reviewers. We strongly encourage code deposition in a community repository (e.g. GitHub). See the Nature Portfolio guidelines for submitting code & software for further information.

Data

Policy information about availability of data

All manuscripts must include a data availability statement. This statement should provide the following information, where applicable:

- Accession codes, unique identifiers, or web links for publicly available datasets
- A description of any restrictions on data availability
- For clinical datasets or third party data, please ensure that the statement adheres to our policy

The 2018 riverbed bathymetry data used in this study were obtained from Vasilopoulos et al.28 and are publicly available at the following URL: https://hydra.hull.ac.uk/resources/hull:17951. The 2013 riverbed bathymetry data were obtained from Hackney et al.30, and are available upon request from the corresponding author of that study. Hydrological data for gauging stations in Cambodia are available through the Mekong River Commission Data Portal: https://

portal.mrcmekong.org/monitoring/river-monitoring-telemetry. Hydrological data for gauging stations in Vietnam can be requested from the Southern Regional Hydro-Meteorological Centre (SRHMC), Vietnam. The 1D model of the Lower Mekong Basin can be requested from the Southern Institute of Water Resources Research (SIWRR), Vietnam.

Research involving human participants, their data, or biological material

Policy information about studies with human participants or human data. See also policy information about sex, gender (identity/presentation), and sexual orientation and race, ethnicity and racism.

Reporting on sex and gender	This study did not involving human participants, their data, or biological material
Reporting on race, ethnicity, or other socially relevant groupings	This study did not involving human participants, their data, or biological material
Population characteristics	This study did not involving human participants, their data, or biological material
Recruitment	This study did not involving human participants, their data, or biological material
Ethics oversight	This study did not involving human participants, their data, or biological material

Note that full information on the approval of the study protocol must also be provided in the manuscript.

Field-specific reporting

Please select the one below that is the best fit for your research. If you are not sure, read the appropriate sections before making your selection.

☐ Life sciences ☐ Behavioural & social sciences ☒ Ecological, evolutionary & environmental sciences

For a reference copy of the document with all sections, see nature.com/documents/nr-reporting-summary-flat.pdf

Ecological, evolutionary & environmental sciences study design

All studies must disclose on these points even when the disclosure is negative.

Study description	This study assesses the impact of riverbed lowering, resulting from sand mining and sediment reduction due to upstream damming, on the seasonal flow reversal from the Mekong River into Tonle Sap Lake
Research sample	Using 1D hydraulic modeling, we assess multiple scenarios of current and future riverbed lowering in the main Mekong River, with variations in upstream water flux conditions based on climate change projections of future monsoon intensity. Specifically, we conducted nine scenarios covering three levels of river bathymetry: (1) a Baseline historical scenario using data measured in 1998, (2) a Contemporary scenario where channel bed levels have decreased by an average of 3.06 m (reflecting observed bed lowering from 1998 to 2018), and (3) a Future scenario projecting continued riverbed lowering over the next 20 years, with an average reduction in bed levels of 5.92 m based on riverbed lowering rates from 1998–2018, projected to 2038. These three bathymetry scenarios were combined with three distinct hydrograph scenarios at the model's upstream boundary (Kratie) to represent historical hydroclimate-driven flow variations from 2000 to 2021: (i) low-water flux conditions with a total volume of 301 billion m^3, (ii) median-water flux conditions with 415 billion m^3, and (iii) high-water flux conditions with 500 billion m^3. These were based on estimated discharge data for 2010, 2009, and 2011, respectively, within the observed dataset from 2000 to 2021.
Sampling strategy	N/A
Data collection	The simulated water levels and discharge at specific locations (Chaktomuk, Preak Kdam, and Kompong Luong) were extracted for each model scenario for analysis and comparison.
Timing and spatial scale	The study area encompasses the entire Lower Mekong basin, extending from Kratie (approximately 540 km from the coast) to the Mekong coast. The simulations were conducted for three periods of riverbed bathymetry: 1998, 2018, and the projected conditions for 2038.
Data exclusions	N/A
Reproducibility	All results presented can be reproduced using the data and model provided in this study.
Randomization	N/A
Blinding	N/A

Did the study involve field work? ☐ Yes ☒ No

Reporting for specific materials, systems and methods

We require information from authors about some types of materials, experimental systems and methods used in many studies. Here, indicate whether each material, system or method listed is relevant to your study. If you are not sure if a list item applies to your research, read the appropriate section before selecting a response.

Materials & experimental systems

n/a	Involved in the study
☒	☐ Antibodies
☒	☐ Eukaryotic cell lines
☒	☐ Palaeontology and archaeology
☒	☐ Animals and other organisms
☒	☐ Clinical data
☒	☐ Dual use research of concern
☒	☐ Plants

Methods

n/a	Involved in the study
☒	☐ ChIP-seq
☒	☐ Flow cytometry
☒	☐ MRI-based neuroimaging

Plants

Seed stocks	N/A
Novel plant genotypes	N/A
Authentication	N/A